Measurement of heart weight and infarct size

After the completion of each experiment, rats were euthanized via anesthetic overdose and the heart excised. The atria were removed and the right ventricle wall separated from the left ventricle and septum. Tissues were blotted and weighed and normalized to 100 g-body weight. The left ventricle was sectioned horizontally through the middle of the infarct area. The apical section of the left ventricle was fixed in 10% buffered formalin and subsequently embedded in paraffin. Sections of the infarcted area, 5 μm thick, were stained with Masons Trichrome stain, mounted for light microscopy examination, and photographed. The infarct size was determined by first measuring the entire endocardial circumference and then measuring the segment of the endocardial circumference that comprised the infarcted portion (14). The infarct size was presented as a percentage of the total left ventricular wall.

Northern blot analysis

Northern blot analysis was performed as previously reported (15) on the basal section of the left ventricle. Total RNA (15 μg/lane) was extracted from rat ventricular tissues using TRIzol (Invitrogen, Carlsbad, CA) reagent, denatured with formaldehyde and formamide, and electrophoresed on 1% agarose gels containing formaldehyde. RNA in the gel was then transferred to a nylon membrane and fixed by UV irradiation. Hybridization of the membrane was performed using ^{32}P-labeled cDNA probes for the mouse atrial natriuretic peptide (ANP), B-type natriuretic peptide (BNP), collagen type I, collagen type III, and glyceraldehyde 3-phosphate dehydrogenase (GAPDH) genes. Band intensity was estimated using a radioimage analyzer (BAS-5000; Fuji Film, Tokyo, Japan). Gene expression was normalized to GAPDH.

Statistical analysis

All statistical analyses were conducted using Statview (version 5.01, SAS Institute, Cary, NC). All results are presented as means ± SEM. One-way ANOVA (factorial) was used to test for differences between groups of rats for each of the measured variables. Where statistical significance was reached, *post hoc* analyses were incorporated using the paired or unpaired *t* test with the Dunnett's correction for multiple comparisons. The Kaplan-Meier survival analysis was performed to compare survival curves between saline-treated and ghrelin-treated rats after LAD coronary artery occlusion. A $P \leq 0.05$ was predetermined as the level of significance for all statistical analyses.

Results

Survival

As shown in Fig. 1, there was a high mortality in the MI rats treated with saline (MI+Saline) (seven of 14 MI rats = 50% mortality). Although mortality rate appeared to be lower in those MI rats treated with ghrelin (MI+Ghrelin) (three of 12 rats = 25%), Kaplan-Meier survival analysis did not reveal any statistical difference ($P = 0.286$). Mortalities associated with the acute MI procedure always occurred within 24 h of the infarct (with one exception), regardless of whether the rat was treated with or without ghrelin. In all cases, the cause of death was attributable to sudden heart failure.

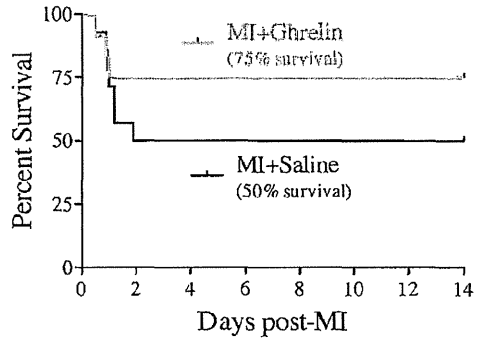

FIG. 1. Kaplan-Meier survival analysis showing the mortality rate in untreated MI+Saline rats (n = 14) compared with ghrelin-treated rats (MI+Ghrelin; n = 12) over 14 d after LAD coronary artery occlusion ($P = 0.286$).

Cardiac sympathetic nerve activity

Fourteen days after the initial MI (or sham) procedure, cardiac SNA (CSNA) was significantly elevated (P = 0.031) in the MI+Saline rats (n = 7) compared with sham rats (n = 7) (Fig. 2A). The 102% increase in CSNA (integrated signal) was largely attributable to an increase in firing rate (*i.e.* Impulses/s; P = 0.019) (Fig. 2B). In contrast, one injection of ghrelin after the initial MI (*i.e.* MI+Ghrelin rats; n = 9) prevented any increase in the CSNA so that basal nerve activity was almost identical to that of sham rats 14 d after the initial MI (Fig. 2B).

Cardiac function (P-V analysis)

Cardiac function was impaired in seven MI+Saline rats 14 d after an acute MI. This was evident by a rightward shift of the left ventricular P-V loop (Fig. 3), compared with sham rats (n = 7), which reflected ventricular dilation (*e.g.* significant 34% increase in LVEDV; $P = 0.007$), an impaired ejection fraction (decrease from 58 to 28%; $P < 0.001$), reduced contractility (35% decrease in dP/dt_{max}; $P = 0.008$), and thus a 35% reduction in both SV and CO ($P = 0.001$, Table 1). Importantly, in those rats that received a single bolus of ghrelin after the acute MI (*i.e.* MI+Ghrelin; n = 9), LVEDV, contractility, SV, and CO were all significantly improved compared with saline-treated MI rats (Table 1). Consequently the magnitude of cardiac dysfunction was attenuated in MI+Ghrelin rats, evident by a smaller rightward shift of the P-V loop (Fig. 3) and a higher ejection fraction (43%; $P = 0.014$). There was no significant difference in mean ABP or HR between all groups of rats (mean ABP range 85–91 mm Hg; HR range 383–387 beats/min).

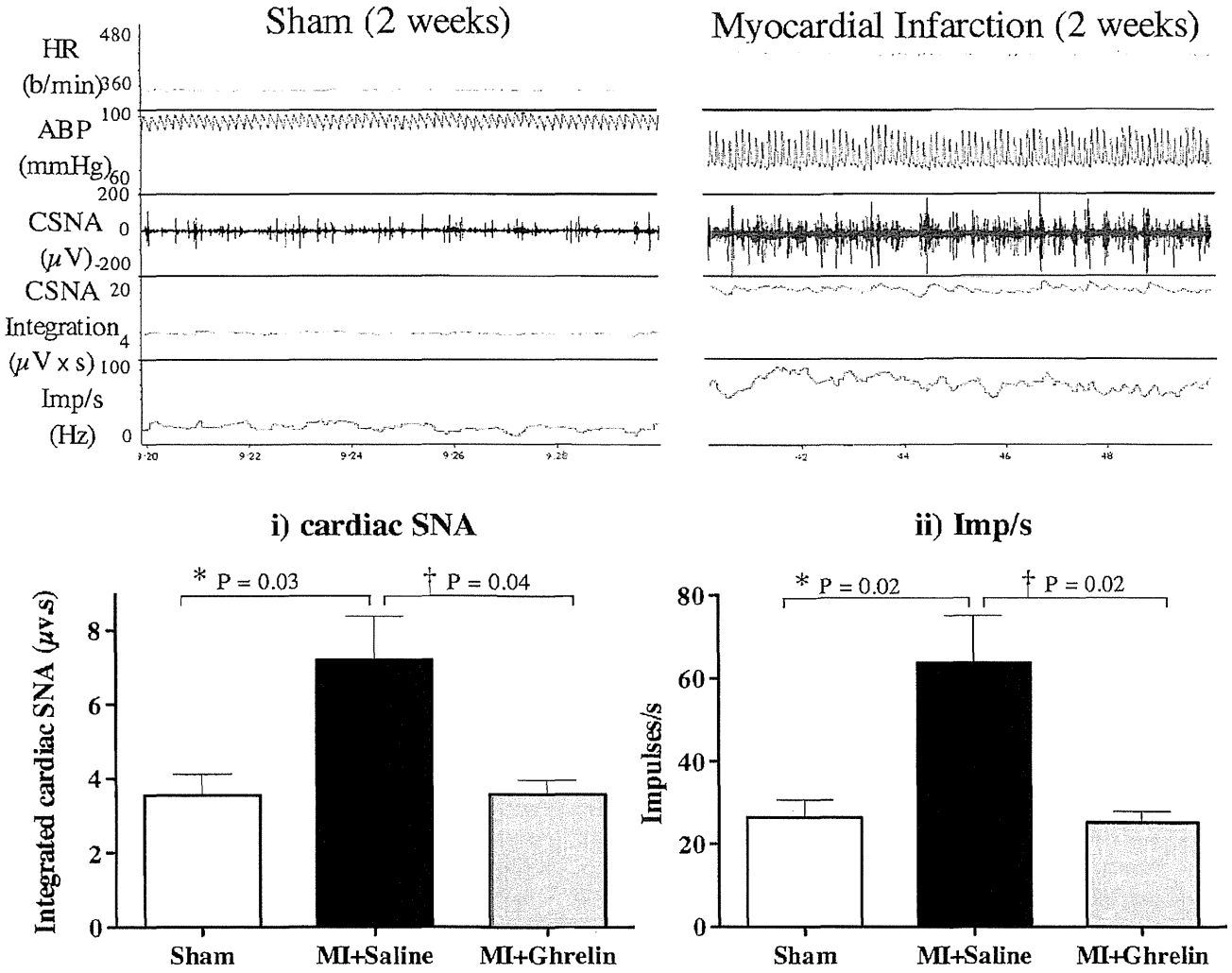

FIG. 2. A, Chart recordings showing raw cardiac SNA (and the derived integrated value and impulses per second) in a rat that had received sham-surgery (SHAM) and a rat that had LAD coronary occlusion surgery (MI) 2 wk previously (no ghrelin treatment). B, Quantitative assessment of cardiac sympathetic nerve activity (i) integration of the raw nerve signal (microvolts per second); ii) impulses per second in sham rats (n = 7), MI+Saline rats (n = 7), and MI+Ghrelin rats (n = 9). *, Significantly different from sham rats; †, significant difference between MI+Saline rats and MI+Ghrelin rats ($P < 0.05$).

mRNA expression analysis

Cardiac dysfunction (*i.e.* MI+Saline rats) was associated with an overexpression of mRNA for genes associated with ventricular remodeling, namely ANP, BNP, and collagen isoforms types I and III ($P < 0.005$; Fig. 4). Importantly, Northern blot (Fig. 4A) and RT-PCR (Fig. 4B) analyses revealed that the overexpression of cardiac remodeling-related genes in MI rats treated with ghrelin, although still statistically significant ($P < 0.01$), was considerably less than that observed in MI+Saline rats.

Heart weight and infarct size

The heart weight of MI+Saline rats had significantly increased by approximately 26% in the 2-wk period after an acute MI ($P < 0.001$), compared with sham rats, reflecting the structural changes (*e.g.* hypertrophy) associated with ventricular remodeling (Table 1). In MI+Ghrelin rats, the magnitude of cardiac hypertrophy, although still significant (11% increase; $P = 0.04$), was attenuated when compared with that of MI+Saline rats (Table 1). The size of the infarct of the left ventricular wall did not significantly differ between MI+Saline rats (37.9 ± 4.4%) and MI+Ghrelin rats (35.6 ± 3.2%).

Discussion

The primary findings of this study highlight that a single bolus of ghrelin, when given within 30 min after an acute MI, prevents an increase in cardiac SNA, which is sustained for at least 2 wk and thus attenuates the magnitude of cardiac dysfunction and remodeling in chronic heart failure.

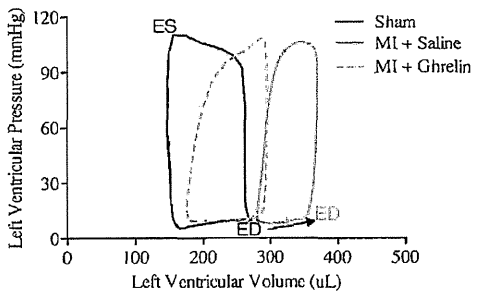

FIG. 3. A graph illustrating the dynamic changes in LVP and LVV (P-V loops) within one complete cardiac cycle, representative for a sham rat, MI+Saline rat, and MI+Ghrelin rats. Note the rightward shift of the P-V loop for the MI+Saline rat, indicative of cardiac dysfunction, which is less apparent in the MI+Ghrelin rats (see Table 1 for collated data from the P-V loops). ED, End diastolic; ES, end systolic.

In a normal heart, SNA plays a pivotal role in modulating ventricular contractility for optimizing CO. Although the increase in cardiac SNA after MI appears to have immediate benefits, providing inotropic support to the heart, this enhanced sympathetic tone is associated with an increased risk of potentially fatal ventricular arrhythmias (1). The enhanced sympathetic tone is then sustained in chronic heart failure (1, 4) and consequently contributes to cardiac dysfunction, remodeling, and increased mortality.

Despite decades of research, the mechanisms for the increase in cardiac SNA after MI remain to be fully elucidated, although stimulation of cardiac reflexes [*e.g.* cardiac vagal and sympathetic afferents (16)], altered peripheral neural reflexes [*e.g.* from chemoreceptors (17)], sympathetic neural remodeling (18), raised levels of hormones [*e.g.* angiotensin II (19)], and changes in central mechanisms that may amplify the responses to these inputs have been implicated (20). What becomes apparent from the plethora of studies in the literature, however, is that the mechanisms that trigger the initial increase in SNA after acute MI may not necessarily be the same mechanisms that sustain the increase in SNA in chronic heart failure.

We have previously reported that ghrelin is able to prevent the early increase in cardiac SNA and thus reduce the incidence of arrhythmias and improve early survival (12). However, we were unable to confirm the duration of ghrelin's effect (beyond 5 h) due to the limitations of an acute anesthetized rat preparation. It stood to reason, however, that once the effects of ghrelin subsided, cardiac SNA would be expected to naturally increase and, ultimately, still adversely exacerbate cardiac dysfunction in chronic heart failure. Yet counterintuitively, the results of this current study indicate that the early administration of ghrelin, which has a plasma half-life of no more than 60 min (21), has a sustained benefit (at least 2 wk) for preventing an adverse increase in cardiac SNA in both acute and chronic heart failure. The obvious question is how can one injection of ghrelin have a sustained effect on cardiac SNA even in chronic heart failure?

Mounting evidence in the literature indicates that ghrelin appears to modulate cardiac SNA via cardiac vagal activation (22), demonstrated by the localization of GHS-R in the vagal nerve terminals in the heart (23), which send afferent projections to the nucleus of the tractus solitarius. As a result, the sympathoinhibitory effects of ghrelin are not evident in vagotomized humans (24). Moreover, ghrelin may also centrally modulate SNA be-

TABLE 1. Indicators of cardiac function in rats 14 d after sham surgery (Sham; n = 7), or MI

	Sham	MI+Saline	MI+Ghrelin
EF (%)	57.9 ± 3.8	27.5 ± 2.6[a]	43.2 ± 1.3[b,c]
SV (μl)	148 ± 7	96 ± 8[a]	126 ± 6[d]
HR (/min)	383 ± 13	387 ± 15	383 ± 14
CO (ml/min)	56.2 ± 1.5	36.8 ± 2.6[a]	48.8 ± 4[d]
LVESP (mm Hg)	122 ± 5	105 ± 5[b]	114 ± 2
LVEDP (mm Hg)	4.07 ± 1.61	6.22 ± 1.26	3.12 ± 1.17[d]
dP/dt_{max} (mm Hg/msec)	11.3 ± 0.9	7.4 ± 0.7[a]	9.4 ± 0.7
dP/dt_{min} (mm Hg/msec)	−7.6 ± 0.8	−5.4 ± 0.5[b]	−5.8 ± 0.2
LVEDV (μl)	262 ± 14	351 ± 19[a]	291 ± 8
LVESV (μl)	113 ± 14	254 ± 18[a]	165 ± 4[b,c]
Heart weight per 100g (mg)	279 ± 8	352 ± 16[a]	311 ± 8[b,d]

MI rats received one bolus of either saline (0.3 ml, MI+saline, n = 7) or ghrelin (150 μg/kg, sc, MI+Ghrelin, n = 9) within 30 min of the infarct. Data are presented as mean ± SEM. EF, Ejection fraction; LVESP, left ventricular end-systolic pressure; LVEDP, left ventricular end-diastolic pressure; LVESV, left ventricular end-systolic volume; dP/dt_{min}, left ventricular pressure fall.

[a] Significantly different from sham rats ($P < 0.01$).

[b] Significantly different from sham rats ($P < 0.05$).

[c] Significant difference between MI+Saline and MI+Ghrelin rats ($P < 0.01$; one way ANOVA).

[d] Significant difference between MI+Saline and MI+Ghrelin rats ($P < 0.05$; one way ANOVA).

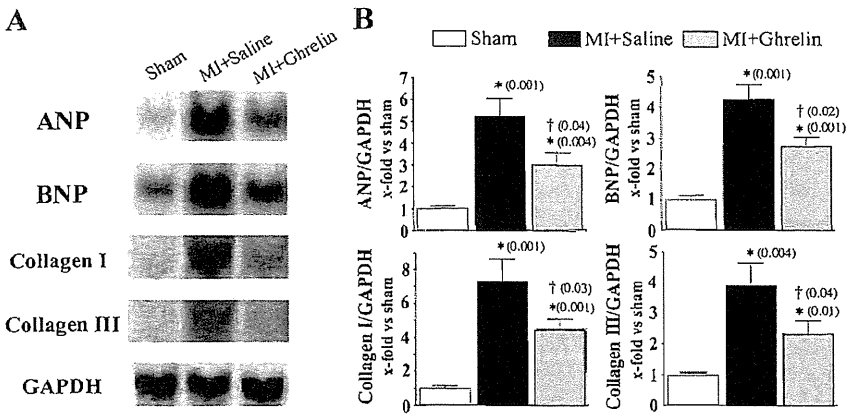

FIG. 4. Ghrelin administration immediately after an acute MI attenuated the overexpression of mRNA for genes associated with cardiac remodeling 2 wk after the initial MI. A, Representative images of Northern blots. B, Quantitative analysis of the Northern blots. Shown are mRNA levels relative to sham-operated rats normalized by GAPDH mRNA levels. *, Significantly different from sham rats; †, significant difference between MI+Saline rats and MI+Ghrelin rats. Statistical *P* values are presented in *parentheses*.

cause the receptors for ghrelin (GHS-R) have been located on neurons of the nucleus tractus solitaries (11), and it has been shown that the central administration of ghrelin directly attenuates renal sympathetic nerve activity (10, 11).

When the administration of ghrelin after an MI is delayed, *i.e.* after 24 h when SNA has already maximally increased (1), ghrelin is still able to transiently reduce sympathetic tone in MI-induced heart failure, although the effect is not sustained without further daily injections (9, 25). It should be noted, however, that aside from its ability to regulate sympathetic tone, chronic ghrelin administration itself is an effective therapeutic strategy in chronic heart failure due to ghrelin's action as a GJRH (26). More recently ghrelin has been shown to promote the use of energy through lipid oxidation (27) and thus attenuate cardiac energy metabolic disturbances (28) in chronic heart failure. Whether an early single bolus dose of ghrelin can chronically enhance cardiac energy utilization is an area that warrants further research.

Although chronic therapeutic interventions are developing for chronic heart failure, it is the period immediately after the infarct, before autonomic modulation of cardiac function becomes irreversibly activated, that appears so critical for optimizing, not only short term but, as this study indicates, also long term outcome by therapeutic intervention.

The underlying mechanism by which one injection of ghrelin is able to sustain a reduced sympathetic tone for 2 wk after MI is unclear, although two possible hypotheses can be considered. First, ghrelin's ability to acutely activate vagal afferents, and hence the parasympathetic nervous system (9), may also provide long-term cytoprotective effects against myocardial injury, through the role of cardiac muscarinic receptors (29). Second, the initial increase in cardiac SNA itself may act as a trigger for instigating the developmental and/or structural changes required for sustaining the increase in SNA. For example, ghrelin, which has been shown to attenuate sympathetic neural remodeling in chronic heart failure (25), may also block the initial step in the cascade of events leading to neural remodeling, if administered soon after an MI, *i.e.* before or soon after cardiac SNA begins to increase. Substantiation of either hypothesis urgently requires further research to identify the potential reflex, signaling, cellular, and/or molecular pathways involved.

Regardless of the underlying mechanisms, the results of this study may impact on our current limited perception of how cardiac function is modulated by the autonomic nervous system in health and, more importantly, in disease. Indeed, there have not been any studies describing the causal relationship between the initial increase in cardiac SNA and the subsequent sustained increase in SNA. It seems that only recently has the central nervous system been considered a significant component in heart failure.

A limitation of this study is that we did not quantify protein content for ANP, BNP, and collagen. Rather, we used the information concerning mRNA expression as an indication, or perhaps prediction, of protein content. Despite this limitation, the fact that ghrelin reduced the overexpression of mRNA for ANP, BNP, and collagen types I and III still remains an important observation with which, hopefully, can advance future directions of research.

Early reperfusion therapy and other recent advances in the treatment of acute MI have substantially reduced mortality and cardiovascular morbidity among MI patients. However, the fact that early arrhythmias can often prove fatal and that acute heart failure and chronic left ventricular remodeling continue to be major determinants of clinical outcome after MI stresses the need for even further advances in therapeutic interventions. In that regard, accumulating clinical and experimental evidence indicates that inhibition of cardiac SNA improves postinfarct survival and mitigates left ventricular remodeling and dysfunction. The current data suggest that one dose of ghrelin dramatically suppress the cardiac SNA early after infarction and may effectively rescue such patients.

In conclusion, this study demonstrates that one dose of ghrelin given in the early stages after an infarct has a long-term benefit of preventing any increase in cardiac SNA and thus attenuates cardiac dysfunction and may potentially have the ability to reduce mortality. The underlying mechanisms governing the long-term effect are unknown, although this study implicates a potential causal interaction between the initial increase in cardiac SNA and the sustained increase in SNA in chronic heart failure. Indeed, autonomic modulation of cardiac function in health and, more importantly, in disease remains poorly understood but offers an effective therapeutic target for improving outcome and thus warrants further research.

Acknowledgments

The authors are grateful for the technical assistance provided by Mrs. Emily Gray and Ms. Isabel Campillo.

Address all correspondence and requests for reprints to: Ichiro Kishimoto, Department of Biochemistry, National Cerebral and Cardiovascular Center Research Institute, 5-7-1 Fujishirodai, Suita, Osaka 565-8565, Japan. E-mail: kishimot@ri.ncvc.go.jp.

This work was supported by the Department of Physiology, University of Otago, New Zealand, and, in part, from the Ministry of Education, Culture, Sports, Science, and Technology of Japan; the Alumni Association of Faculty of Medicine, Kagawa University, Grant 22-2; the Banyu Life Science Foundation International; the ONO Medical Research Foundation; and the Takeda Science Foundation.

Disclosure Summary: The authors have nothing to disclose.

References

1. Jardine DL, Charles CJ, Ashton RK, Bennett SI, Whitehead M, Frampton CM, Nicholls MG 2005 Increased cardiac sympathetic nerve activity following acute myocardial infarction in a sheep model. J Physiol 565:325–333
2. Huang BS, Leenen FH 2009 The brain renin-angiotensin-aldosterone system: a major mechanism for sympathetic hyperactivity and left ventricular remodeling and dysfunction after myocardial infarction. Curr Heart Fail Rep 6:81–88
3. Tsukamoto T, Morita K, Naya M, Inubushi M, Katoh C, Nishijima K, Kuge Y, Okamoto H, Tsutsui H, Tamaki N 2007 Decreased myocardial β-adrenergic receptor density in relation to increased sympathetic tone in patients with nonischemic cardiomyopathy. J Nucl Med 48:1777–1782
4. Lymperopoulos A, Rengo G, Gao E, Ebert SN, Dorn 2nd GW, Koch WJ 2010 Reduction of sympathetic activity via adrenal-targeted GRK2 gene deletion attenuates heart failure progression and improves cardiac function after myocardial infarction. J Biol Chem 285:16378–16386
5. Kojima M, Hosoda H, Date Y, Nakazato M, Matsuo H, Kangawa K 1999 Ghrelin is a growth-hormone-releasing acylated peptide from stomach. Nature 402:656–660
6. Pusztai P, Sarman B, Ruzicska E, Toke J, Racz K, Somogyi A, Tulassay Z 2008 Ghrelin: a new peptide regulating the neurohormonal system, energy homeostasis and glucose metabolism. Diabetes Metab Res Rev 24:343–352
7. Nagaya N, Uematsu M, Kojima M, Ikeda Y, Yoshihara F, Shimizu W, Hosoda H, Hirota Y, Ishida H, Mori H, Kangawa K 2001 Chronic administration of ghrelin improves left ventricular dysfunction and attenuates development of cardiac cachexia in rats with heart failure. Circulation 104:1430–1435
8. Nagaya N, Kangawa K 2003 Ghrelin improves left ventricular dysfunction and cardiac cachexia in heart failure. Curr Opin Pharmacol 3:146–151
9. Soeki T, Kishimoto I, Schwenke DO, Tokudome T, Horio T, Yoshida M, Hosoda H, Kangawa K 2008 Ghrelin suppresses cardiac sympathetic activity and prevents early left ventricular remodeling in rats with myocardial infarction. Am J Physiol Heart Circ Physiol 294:H426–H432
10. Matsumura K, Tsuchihashi T, Fujii K, Abe I, Iida M 2002 Central ghrelin modulates sympathetic activity in conscious rabbits. Hypertension 40:694–699
11. Lin Y, Matsumura K, Fukuhara M, Kagiyama S, Fujii K, Iida M 2004 Ghrelin acts at the nucleus of the solitary tract to decrease arterial pressure in rats. Hypertension 43:977–982
12. Schwenke DO, Tokudome T, Kishimoto I, Horio T, Shirai M, Cragg PA, Kangawa K 2008 Early ghrelin treatment after myocardial infarction prevents an increase in cardiac sympathetic tone and reduces mortality. Endocrinology 149:5172–5176
13. Pacher P, Nagayama T, Mukhopadhyay P, Bátkai S, Kass DA 2008 Measurement of cardiac function using pressure-volume conductance catheter technique in mice and rats. Nature Prorocols 3:1422–1434
14. Pfeffer MA, Pfeffer JM, Fishbein MC, Fletcher PJ, Spadaro J, Kloner RA, Braunwald E 1979 Myocardial infarct size and ventricular function in rats. Circ Res 44:503–512
15. Schwenke DO, Tokudome T, Shirai M, Hosoda H, Horio T, Kishimoto I, Kangawa K 2008 Exogenous ghrelin attenuates the progression of chronic hypoxia-induced pulmonary hypertension in conscious rats. Endocrinology 149:237–244
16. Fu LW, Longhurst JC 2009 Regulation of cardiac afferent excitability in ischemia. In: Canning BJ, Spina D, eds. Handbook of Experimental Pharmacology. Berlin: Springer-Velag; 185–225
17. Schultz HD, Li YL 2007 Carotid body function in heart failure. Respir Physiol Neurobiol 157:171–185
18. Liu YB, Wu CC, Lu LS, Su MJ, Lin CW, Lin SF, Chen LS, Fishbein MC, Chen PS, Lee YT 2003 Sympathetic nerve sprouting, electrical remodeling, and increased vulnerability to ventricular fibrillation in hypercholesterolemic rabbits. Circ Res 92:1145–1152
19. Shi Z, Chen AD, Xu Y, Chen Q, Gao XY, Wang W, Zhu GQ 2009 Long-term administration of tempol attenuates postinfarct ventricular dysfunction and sympathetic activity in rats. Pflugers Arch 458:247–257
20. Watson AM, Hood SG, May CN 2006 Mechanisms of sympathetic activation in heart failure. Clin Exp Pharmacol Physiol 33:1269–1274
21. Blatnik M, Soderstrom CI 2011 A practical guide for the stabilization of acylghrelin in human blood collections. Clin Endocrinol (Oxf) 74:325–331
22. Shimizu S, Akiyama T, Kawada T, Sonobe T, Kamiya A, Shishido T, Tokudome T, Hosoda H, Shirai M, Kangawa K, Sugimachi M 2011 Centrally administered ghrelin activates cardiac vagal nerve in anesthetized rabbits. Auton Neurosci 162:60–65
23. Kishimoto I, Tokudome T, Schwenke D, Soeki T, Hosoda H, Nagaya N, Kangawa K 2009 Therapeutic potential of ghrelin in cardiac diseases. Exp Rev Endocrinol Metab 4:283–289
24. Huda MS, Mani H, Dovey T, Halford JC, Boyland E, Daousi C, Wilding JP, Pinkney J 2010 Ghrelin inhibits autonomic function in

healthy controls, but has no effect on obese and vagotomized subjects. Clin Endocrinol (Oxf) 73:678–685
25. Yuan MJ, Huang CX, Tang YH, Wang X, Huang H, Chen YJ, Wang T 2009 A novel peptide ghrelin inhibits neural remodeling after myocardial infarction in rats. Eur J Pharmacol 618:52–57
26. Nagaya N, Moriya J, Yasumura Y, Uematsu M, Ono F, Shimizu W, Ueno K, Kitakaze M, Miyatake K, Kangawa K 2004 Effects of ghrelin administration on left ventricular function, exercise capacity, and muscle wasting in patients with chronic heart failure. Circulation 110:3674–3679
27. Andrews ZB, Erion DM, Beiler R, Choi CS, Shulman GI, Horvath TL 2010 Uncoupling protein-2 decreases the lipogenic actions of ghrelin. Endocrinology 151:2078–2086
28. Xu JP, Wang HX, Wang W, Zhang LK, Tang CS 2010 Ghrelin improves disturbed myocardial energy metabolism in rats with heart failure induced by isoproterenol. J Pept Sci 16:392–402
29. Yang B, Lin H, Xu C, Liu Y, Wang H, Han H, Wang Z 2005 Choline produces cytoprotective effects against ischemic myocardial injuries: evidence for the role of cardiac m3 subtype muscarinic acetylcholine receptors. Cell Physiol Biochem 16:163–174

BASIC RESEARCH www.jasn.org

Natriuretic Peptide Receptor Guanylyl Cyclase-A Protects Podocytes from Aldosterone-Induced Glomerular Injury

Yoshihisa Ogawa,* Masashi Mukoyama,* Hideki Yokoi,* Masato Kasahara,* Kiyoshi Mori,* Yukiko Kato,* Takashige Kuwabara,* Hirotaka Imamaki,* Tomoko Kawanishi,* Kenichi Koga,* Akira Ishii,* Takeshi Tokudome,† Ichiro Kishimoto,‡ Akira Sugawara,* and Kazuwa Nakao*

*Department of Medicine and Clinical Science, Kyoto University Graduate School of Medicine, Kyoto, Japan; †Department of Biochemistry, National Cerebral and Cardiovascular Research Institute, Osaka, Japan; and ‡Department of Atherosclerosis and Diabetes, National Cerebral and Cardiovascular Center, Osaka, Japan

ABSTRACT

Natriuretic peptides produced by the heart in response to cardiac overload exert cardioprotective and renoprotective effects by eliciting natriuresis, reducing BP, and inhibiting cell proliferation and fibrosis. These peptides also antagonize the renin-angiotensin-aldosterone system, but whether this mechanism contributes to their renoprotective effect is unknown. Here, we examined the kidneys of mice lacking the guanylyl cyclase-A (GC-A) receptor for natriuretic peptides under conditions of high aldosterone and high dietary salt. After 4 weeks of administering aldosterone and a high-salt diet, GC-A knockout mice, but not wild-type mice, exhibited accelerated hypertension with massive proteinuria. Aldosterone-infused GC-A knockout mice had marked mesangial expansion, segmental sclerosis, severe podocyte injury, and increased oxidative stress. Reducing the BP with hydralazine failed to lessen such changes; in contrast, blockade of the renin-angiotensin-aldosterone system markedly reduced albuminuria, ameliorated podocyte injury, and reduced oxidative stress. Furthermore, treatment with the antioxidant tempol significantly reduced albuminuria and abrogated the histologic changes. In cultured podocytes, natriuretic peptides inhibited aldosterone-induced mitogen-activated protein kinase phosphorylation. Taken together, these results suggest that renoprotective properties of the endogenous natriuretic peptide/GC-A system may result from the local inhibition of the renin-angiotensin-aldosterone system and oxidative stress in podocytes.

J Am Soc Nephrol 23: 1198–1209, 2012. doi: 10.1681/ASN.2011100985

Aldosterone, beyond its effects on sodium reabsorption, has been shown to play an important role in causing cardiovascular complications including renal injury.[1,2] Proteinuria is not rare in patients with primary aldosteronism, suggesting that aldosterone can induce renal injury independent of circulating angiotensin II (AngII) levels.[3] In experimental nephropathy models, aldosterone exerts direct effects on renal cells, leading to the progression of glomerulosclerosis and proteinuria.[4] Several studies have revealed positive feedback by which aldosterone activates the renin-angiotensin-aldosterone system (RAAS), through inducing renin and angiotensin-converting enzyme gene expression,[5,6] or by activating AngII type 1 (AT1) receptor signaling.[7] Furthermore, aldosterone upregulates reactive oxygen species (ROS) and activates mitogen-activated protein kinases (MAPKs) in the kidney and cardiovascular system.[7–9]

Podocytes play a crucial role in barrier function as well as the pathogenesis of glomerular diseases, forming a branched interdigitating network with foot processes by the slit diaphragm.[10] Genetic

Received October 13, 2011. Accepted April 15, 2012.

Published online ahead of print. Publication date available at www.jasn.org.

Correspondence: Dr. Masashi Mukoyama, Department of Medicine and Clinical Science, Kyoto University Graduate School of Medicine, 54 Shogoin Kawahara-cho, Sakyo-ku, Kyoto 606-8507, Japan. Email: muko@kuhp.kyoto-u.ac.jp

studies have proved roles of slit diaphragm–associated proteins, including nephrin and podocin, in various proteinuric disorders.[10] Recently, podocytes have attracted greater attention as the target for aldosterone action. In fact, aldosterone causes foot process effacement and downregulation of nephrin and podocin, via the mineralocorticoid receptor.[7,11–13] In addition, the mineralocorticoid receptor in podocytes can be activated by Rac1 GTPase, which is sufficient to cause glomerular injury and proteinuria irrespective of aldosterone levels.[13]

The natriuretic peptide family consisting of atrial natriuretic peptide (ANP), brain natriuretic peptide (BNP), and C-type natriuretic peptide possess potent diuretic, natriuretic, and vasodilating properties.[14] ANP and BNP are secreted predominantly by the cardiac atrium and ventricle, respectively, upon cardiac overload.[14–16] They exert various biologic effects by acting on guanylyl cyclase-A (GC-A)/natriuretic peptide receptor-A (NPR-A), which is the major and possibly the only receptor for ANP and BNP, through the activation of cGMP/cGMP-dependent protein kinase.[17] GC-A is abundantly expressed in blood vessels and the heart[17]; within the kidney, it is localized in glomeruli, thin limbs of Henle's loop, cortical collecting ducts, and inner medullary collecting ducts.[18] In glomeruli, GC-A is expressed in mesangial cells and podocytes.[18] GC-A–deficient mice show chronic salt-independent elevation of BP by approximately 15–30 mmHg[19] and cardiac hypertrophy,[20] with virtually no natriuretic or diuretic response to acute volume expansion.[21] These studies clearly demonstrate essential roles for natriuretic peptide/GC-A signaling in BP regulation and acute volume handling through the kidney, but the role of GC-A in podocyte injury remains elusive.

A renoprotective action of ANP has been shown early using animal models of ARF.[22] A recent meta-analysis reveals that the administration of low-dose ANP may exert beneficial effects in clinical AKI.[23] We previously showed that chronic excess of BNP in mice prevents glomerular injury after subtotal nephrectomy,[24] and ameliorates proteinuria and histologic changes in immune-mediated renal injury[25] as well as in diabetic nephropathy.[26] In addition to exerting direct vasodilating and diuretic actions, natriuretic peptides act to antagonize the RAAS at multiple steps.[14,27,28] We postulate therefore that the beneficial effects of natriuretic peptides should be brought about, at least in part, by antagonizing local activation and/or action of the RAAS in the kidney.[24–26]

To explore the role of natriuretic peptide/GC-A signaling in aldosterone-induced renal injury, we investigated renal findings of mice deficient in GC-A, along with the challenge of aldosterone and a high-salt diet.

RESULTS

Aldosterone Infusion Causes Accelerated Hypertension in GC-A Knockout Mice

All mice were uninephrectomized and fed with 6% NaCl, with or without aldosterone infusion (0.2 μg/kg body weight per minute) for 4 weeks. Changes in systolic BP (SBP) in each group are shown in Figure 1 (time courses shown in Supplemental Figure 1). Aldosterone infusion in wild-type mice resulted in marginally higher SBP than vehicle (118.1±3.3 versus 116.6±4.5 mmHg at 4 weeks). GC-A knockout mice showed a significantly higher SBP compared with wild-type mice at baseline (126.2±2.7 versus 110.4±3.3 mmHg, $P<0.05$), and revealed marked hypertension after aldosterone infusion compared with vehicle (159.0±6.6 versus 123.0±4.5 mmHg at 4 weeks, $P<0.01$). Administration of hydralazine, spironolactone, or olmesartan in aldosterone-infused GC-A knockout mice resulted in reduced SBP to the same degree (135.7±3.1, 135.2±8.0, and 140.0±5.2 mmHg, respectively). In contrast, there was no significant SBP change with tempol (151.1±6.9 mmHg).

Body and Kidney Weights and Blood Parameters

Body weights and kidney weights are presented in Supplemental Table 1. GC-A knockout mice showed normal kidney weight at baseline but exhibited renal hypertrophy compared with wild-type mice as indicated by an increase in kidney weight per body weight at 4 weeks. Aldosterone infusion caused renal hypertrophy in both wild-type and GC-A knockout mice, and administration of spironolactone ameliorated such changes in GC-A knockout mice.

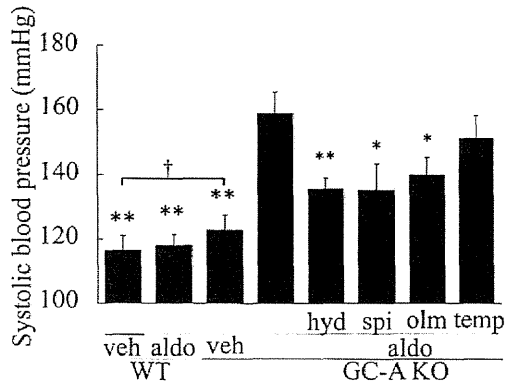

Figure 1. The comparison in SBP at 4 weeks after aldosterone or vehicle infusion. Data are from vehicle-infused wild-type mice (WT veh, n=5), aldosterone-infused wild-type mice (WT aldo, n=8), vehicle-infused GC-A knockout mice (GC-A KO veh, n=5), aldosterone-infused GC-A knockout mice (GC-A KO aldo, n=8), aldosterone-infused GC-A knockout mice treated with hydralazine (KO aldo+hyd, n=6), those treated with spironolactone (KO aldo +spi, n=5), those treated with olmesartan (KO aldo+olm, n=5), and those treated with tempol (KO aldo+temp, n=5). Aldosterone-infused GC-A knockout mice exhibited marked hypertension, and administration of hydralazine, spironolactone, or olmesartan in aldosterone-infused GC-A knockout mice resulted in reduced SBP to the same degree. In contrast, there was no significant SBP change with tempol. *$P<0.05$, **$P<0.01$, versus KO aldo, †$P<0.05$. WT, wild-type; veh, vehicle; aldo, aldosterone; KO, knockout; hyd, hydralazine; spi, spironolactone; olm, olmesartan; temp, tempol.

Serum aldosterone was markedly high (approximately 70-fold) and serum potassium was low in all aldosterone-infused groups (Supplemental Table 1). There was no significant difference in serum aldosterone, potassium, or creatinine levels among aldosterone-infused groups.

Aldosterone Causes Massive Proteinuria in GC-A Knockout Mice

At the basal level (−2 weeks), urinary albumin excretion was not different between wild-type and GC-A knockout mice (38.7±4.9 and 41.4±4.8 μg/mgCr, respectively) (Figure 2A). Aldosterone-infused wild-type mice showed a three-fold increase in urinary albumin excretion at 4 weeks compared with vehicle (129.2±25.4 versus 43.0±6.6 μg/mgCr, $P<0.01$). Surprisingly, aldosterone-infused GC-A knockout mice revealed 260 times higher urinary albumin excretion than vehicle-infused GC-A knockout mice at 4 weeks (17,559±6845 μg/mgCr versus 67.2±24.4 μg/mgCr, $P<0.01$). Administration of hydralazine in these mice significantly reduced BP, but failed to suppress albuminuria (Figure 2B). In contrast, spironolactone administration markedly reduced urinary albumin excretion by 95% in aldosterone-infused GC-A knockout mice (1069±411 μg/mgCr). Moreover, treatment with an angiotensin receptor blocker (ARB) olmesartan significantly reduced urinary albumin excretion by 70% (5450±1765 μg/mgCr). Treatment with tempol also reduced albuminuria by 60% (7125±2292 μg/mgCr). These results suggest that, in the absence of GC-A signaling, aldosterone stimulation can activate the renin-angiotensin system and oxidative stress in the kidney, leading to massive proteinuria.

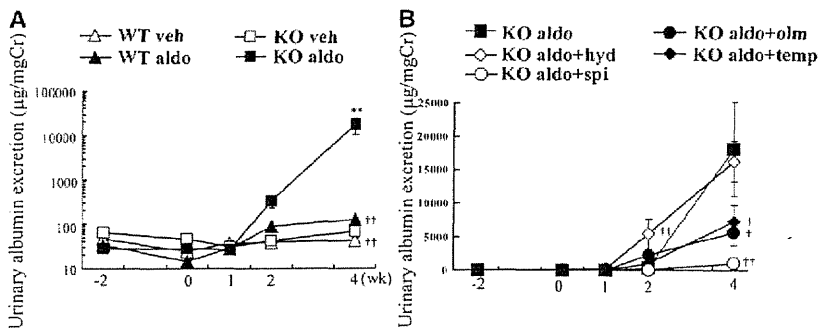

Figure 2. Urinary albumin excretion in wild-type or GC-A knockout mice with or without aldosterone. (A) Aldosterone infusion resulted in a marked increase of albuminuria in GC-A knockout mice. Data from wild-type mice with vehicle (WT veh, open triangles), wild-type mice with aldosterone (WT aldo, filled triangles), GC-A knockout mice with vehicle (KO veh, open squares), and GC-A knockout mice with aldosterone (KO aldo, filled squares) are shown. (B) Administration of spironolactone (spi, open circles), olmesartan (olm, filled circles), or tempol (temp, filled diamonds) significantly reduced albuminuria in aldosterone-infused GC-A knockout mice. Hydralazine (hyd, open diamonds) did not reduce albuminuria. WT veh, n=5; WT aldo, n=8; KO veh, n=5; KO aldo, n=8; KO aldo+hyd, n=6; KO aldo+spi, n=5; KO aldo+olm, n=5; and KO aldo+temp, n=5. $^{**}P<0.01$, KO veh versus KO aldo, $^{\dagger}P<0.05$, $^{\dagger\dagger}P<0.01$, versus KO aldo.

Renal Histologic Changes in Aldosterone-Infused GC-A Knockout Mice

We examined renal histology at 4 weeks after aldosterone administration. In superficial glomeruli, aldosterone-infused wild-type mice exhibited marginal mesangial expansion with mild glomerular hypertrophy (Figure 3A). Renal histology of GC-A knockout mice showed virtually no significant difference from that of wild-type mice at baseline; after aldosterone infusion, GC-A knockout mice exhibited marked mesangial expansion with glomerular hypertrophy (Figure 3, A and B and Supplemental Figure 2A). Although hydralazine administration failed to ameliorate such changes, treatment with spironolactone, olmesartan, or tempol resulted in inhibited mesangial expansion in these mice.

In juxtamedullary glomeruli, there were minor glomerular abnormalities in aldosterone-infused wild-type mice; in contrast, aldosterone-infused GC-A knockout mice exhibited severe segmental sclerosis and marked glomerular hypertrophy (Figure 3C). Again, these changes were unaltered with hydralazine but were alleviated with spironolactone, olmesartan, or tempol (Figure 3D and Supplemental Figure 2B). The number of sclerotic glomeruli was also significantly reduced with spironolactone, olmesartan, or tempol (Figure 3E). Localization of GC-A was examined by immunohistochemistry. Wild-type mice revealed the presence of GC-A presumably at podocytes, distal tubules, and collecting ducts, which was apparently unaltered with aldosterone infusion (Figure 3F).

We next examined renal fibrotic changes in these mice (Figure 4). Whereas wild-type mice with aldosterone showed slight fibrotic changes with mild tubular atrophy, aldosterone-infused GC-A knockout mice exhibited tubular dilation with marked protein cast deposition and significant tubulointerstitial fibrosis. These changes were not changed with hydralazine but ameliorated with spironolactone, olmesartan, and less effectively with tempol (Figure 4, A and B).

Podocyte Injury in Aldosterone-Infused GC-A Knockout Mice

We then evaluated podocyte injury in these mice. Electron microscopic analyses revealed that wild-type mice with aldosterone exhibited slightly widened podocyte foot processes without thickening of the glomerular basement membrane (GBM) (Figure 5). Vehicle-infused GC-A knockout mice showed thickened GBM without widening of foot processes. GC-A knockout mice with aldosterone showed foot process effacement with irregular thickening of GBM, and these changes were not improved with hydralazine, but reversed with spironolactone and

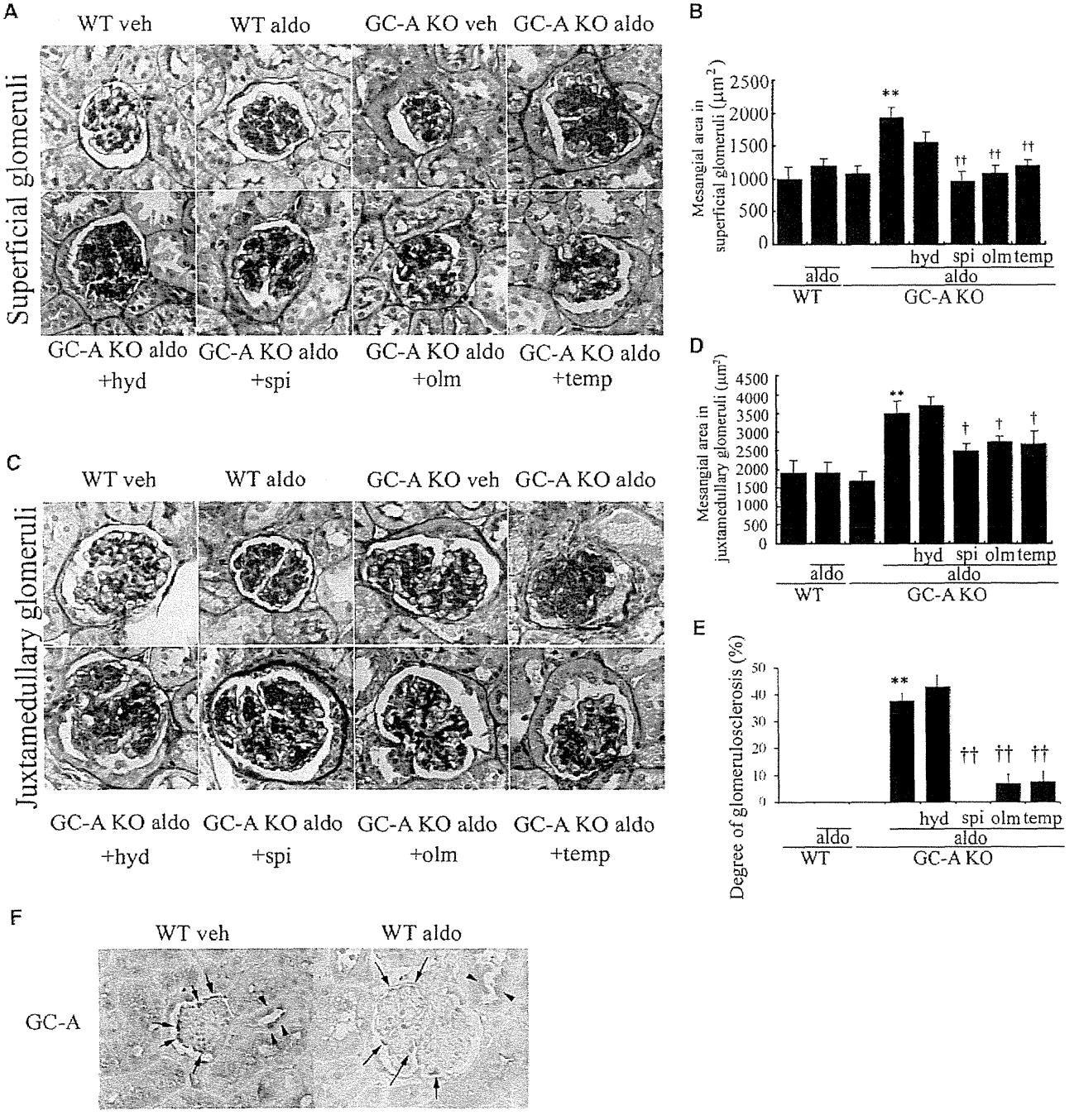

Figure 3. Histologic examination of glomeruli in aldosterone-infused GC-A knockout mice and the localization of GC-A. Light microscopic analyses were performed at 4 weeks after aldosterone administration, stained with periodic acid-Schiff. (A) Representative views of superficial glomeruli. Aldosterone-infused wild-type mice (WT aldo) showed marginal mesangial expansion with mild glomerular hypertrophy. Aldosterone-infused GC-A knockout mice (GC-A KO aldo) exhibited marked mesangial expansion with glomerular hypertrophy. Administration of hydralazine in GC-A knockout mice (GC-A KO aldo+hyd) did not affect glomerular changes. Administration of spironolactone (GC-A KO aldo+spi), olmesartan (GC-A KO aldo+olm), or tempol (GC-A KO aldo+temp) in GC-A knockout mice improved histologic changes. (B) Mesangial area in superficial glomeruli at 4 weeks. (C) Representative views of juxtamedullary glomeruli. Aldosterone-infused GC-A knockout mice showed severe segmental sclerosis and marked glomerular hypertrophy. Administration of spironolactone, olmesartan or tempol ameliorated glomerular changes. (D) Mesangial area in juxtamedullary glomeruli at 4 weeks. (E) Degree of glomerulosclerosis in juxtamedullary glomeruli. (F) Immunohistochemical study for GC-A. GC-A was positive at podocytes (arrows) and distal tubules (arrowheads). WT veh, n=5; WT aldo, n=8; KO veh, n=5; KO aldo, n=8; KO aldo+hyd, n=6; KO aldo+spi, n=5; KO aldo+olm, n=5; and KO aldo+temp, n=5. $^{**}P<0.01$, KO veh versus KO aldo, $^{\dagger}P<0.05$, $^{\dagger\dagger}P<0.01$, versus KO aldo. WT, wild-type; veh, vehicle; aldo, aldosterone; KO, knockout; hyd, hydralazine; spi, spironolactone; olm, olmesartan; temp, tempol.

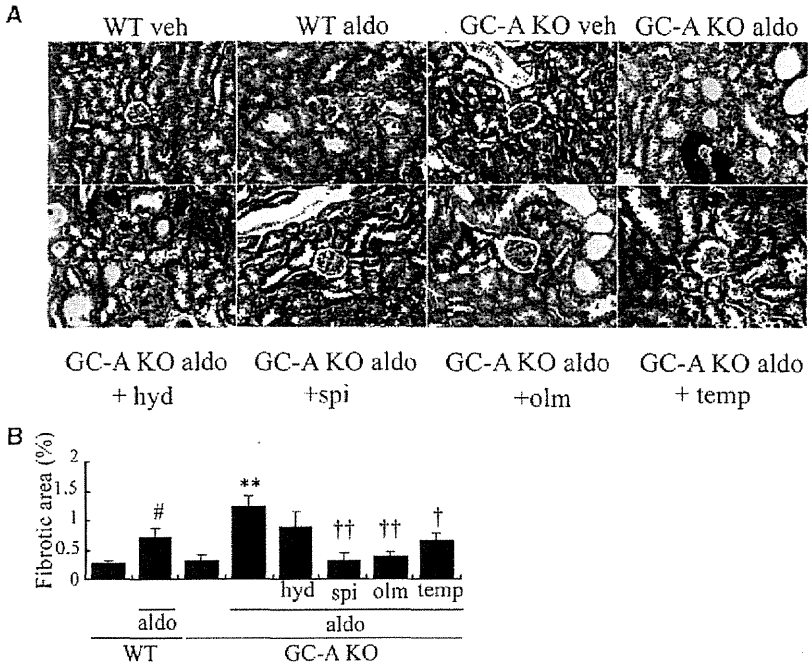

Figure 4. Histologic examination of tubulointerstitial fibrosis by Masson's trichrome-stained sections at 4 weeks. (A) Representative views of tubules and interstitial fibrosis. Aldosterone-infused wild-type mice (WT aldo) showed mild tubulointerstitial fibrosis with tubular atrophy. Aldosterone-infused GC-A knockout mice (GC-A KO aldo) exhibited tubular dilation with protein casts and tubulointerstitial fibrosis. These changes were not improved with hydralazine (GC-A KO aldo+hyd), but ameliorated with spironolactone (GC-A KO aldo+spi), olmesartan (GC-A KO aldo+olm), or tempol (GC-A KO aldo+temp). (B) Fibrotic area at 4 weeks. WT veh, n=5; WT aldo, n=8; KO veh, n=5; KO aldo, n=8; KO aldo+hyd, n=6; KO aldo+spi, n=5; KO aldo+olm, n=5; and KO aldo +temp, n=5. $^{\#}P<0.05$, WT veh versus WT aldo, $^{**}P<0.01$, KO veh versus KO aldo, $^{\dagger}P<0.05$, $^{\dagger\dagger}P<0.01$, versus KO aldo. WT, wild-type; veh, vehicle; aldo, aldosterone; KO, knockout; hyd, hydralazine; spi, spironolactone; olm, olmesartan; temp, tempol.

also lessened with olmesartan (Figure 5, A and B). Tempol administration improved width of foot processes.

The expression of podocyte markers nephrin and podocin was decreased in aldosterone-infused GC-A knockout mice at 4 weeks with or without hydralazine, and such changes were ameliorated with spironolactone, olmesartan, or tempol (Figure 6, A and B).

Gene Expression and ROS in Glomeruli of Aldosterone-Infused GC-A Knockout Mice

Analyses on glomerular expression of extracellular matrix (ECM)–related genes (Figure 7A) revealed that TGF-β1 mRNA was enhanced with aldosterone both in wild-type and in GC-A knockout mice. Such upregulation was significantly reduced with spironolactone or tempol, and tended to decrease with olmesartan treatment. Similar tendency was observed in connective tissue growth factor, fibronectin, and collagen 1 and 4 mRNA expressions (Figure 7A and Supplemental Figure 3).

We next examined the expression of NADPH oxidase 2 (Nox-2) or gp91phox/Cybb, p22phox/Cyba, and Nox-4, which are essential membrane components of NADPH oxidase.[29] Aldosterone infusion upregulated the glomerular expression of gp91phox/Cybb mRNA, and less potently that of p22phox and Nox-4 (Figure 7B and Supplemental Figure 3). Treatment with spironolactone or tempol significantly reduced them. Immunohistochemical study for 8-hydroxydeoxyguanosine (8-OHdG) showed that aldosterone infusion exhibited strong staining mainly at podocytes and tubular cells only in GC-A knockout mice (Figure 7, C and D). Such upregulation was significantly reduced with spironolactone, olmesartan, or tempol, but not with hydralazine.

Enhanced Phosphorylation of MAPKs in Aldosterone-Infused GC-A Knockout Mice

We found a mild increase of phosphorylated extracellular signal-regulated kinase (ERK) in glomeruli of aldosterone-infused wild-type mice (Figure 8A). Phosphorylation of ERK in glomeruli was pronounced in aldosterone-infused GC-A knockout mice. Double immunostaining revealed that the cells expressing phospho-ERK were also positive for Wilms' tumor 1 (WT1), a podocyte marker (Figure 8B). Phosphorylation of ERK was reduced by treatment with spironolactone, olmesartan, or tempol, but not with hydralazine (Figure 8, C and D). Essentially similar results were obtained as to phospho-p38 MAPK-positive cells, which were double stained with WT1 (Figure 8, E and F); the phosphorylation of p38 MAPK was reduced with spironolactone or olmesartan, and also with tempol (Figure 8, E, G, and H).

ANP Inhibits Phosphorylation of ERK and p38 MAPK in Cultured Mouse Podocytes

We examined the effect of ANP on phosphorylation of ERK and p38 MAPK in cultured mouse podocytes. Aldosterone caused the phosphorylation of ERK as quickly as 10 minutes after the stimulation and lasted for as long as 30 minutes (Figure 9A). Pretreatment with ANP completely abolished ERK phosphorylation (Figure 9B). The phosphorylation of p38 MAPK was upregulated at 3 hours after aldosterone stimulation, and such induction was significantly inhibited with ANP treatment (Figure 9, C and D).

GC-A knockdown in podocytes showed higher levels of phosphorylated ERK and p38 MAPK than controls (Supplemental Figure 4). Treatment with olmesartan or spironolactone, but not tempol, partially decreased phospho-ERK; cGMP analog strongly reduced phosphorylation of both ERK and p38 MAPK (Supplemental Figure 4). Cultured podocytes stimulated

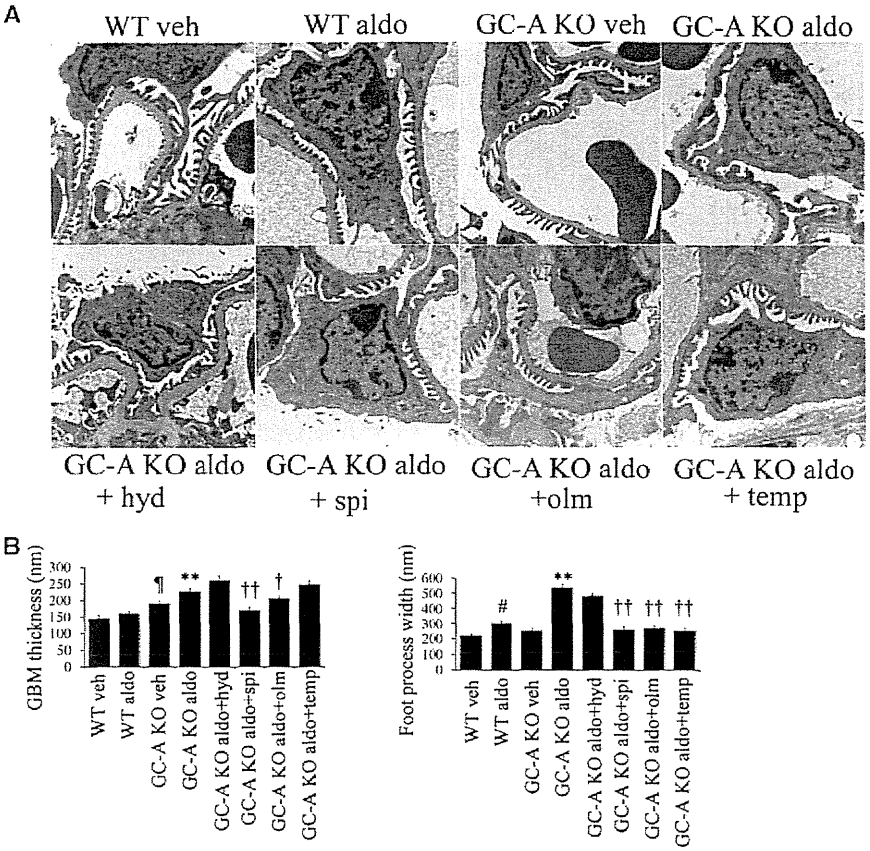

Figure 5. Electron microscopic analyses of glomeruli in aldosterone-infused GC-A knockout mice at 4 weeks. (A) Aldosterone-infused wild-type mice (WT aldo) showed almost normal foot process structure. Vehicle-infused GC-A knockout mice (GC-A KO veh) had normal podocyte foot processes. Aldosterone-infused GC-A knockout mice (GC-A KO aldo) showed foot process effacement with irregular thickening of glomerular basement membrane. These changes were not improved with administration of hydralazine (GC-A KO aldo+hyd), but ameliorated with spironolactone (GC-A KO aldo+spi), olmesartan (GC-A KO aldo+olm), or tempol (GC-A KO aldo+temp). (B) GBM thickness and foot process width (n=3, each). $^{\#}P<0.05$, WT veh versus WT aldo, $^{**}P<0.01$, KO veh versus KO aldo, $^{\dagger}P<0.05$, $^{\dagger\dagger}P<0.01$, versus KO aldo, $^{\P}P<0.05$, KO veh versus WT veh. WT, wild-type; veh, vehicle; aldo, aldosterone; KO, knockout; hyd, hydralazine; spi, spironolactone; olm, olmesartan; temp, tempol.

with aldosterone upregulated expression of connexin43 (Gja1), a podocyte injury marker. This upregulation was significantly inhibited by the treatment with MAPK kinase (MEK) inhibitor U0126 or p38 MAPK inhibitor SB203580 (Figure 9E). Finally, we confirmed whether aldosterone action was mediated through a mineralocorticoid receptor. Upregulation of connexin43 mRNA in aldosterone-stimulated podocytes was not reduced by glucocorticoid receptor blocker mifepristone, but by spironolactone (Figure 9F).

DISCUSSION

We investigated the role of the natriuretic peptide/GC-A system in aldosterone-induced renal injury. Although aldosterone administration in wild-type mice resulted in minor glomerular abnormalities with marginal increase of albuminuria, GC-A–deficient mice exhibited accelerated hypertension and severe glomerulopathy with massive proteinuria, indicating that GC-A signaling should normally act to inhibit aldosterone-induced glomerular injury. We must be cautious to interpret BP by tail-cuff manometry, because it is not as precise as direct monitoring. Nevertheless, these actions were not merely BP dependent, and we therefore hypothesized that GC-A signaling works at podocytes in this model. In fact, aldosterone exerted marked podocyte injury, only in the absence of GC-A.

Besides massive proteinuria, aldosterone caused glomerulosclerosis and interstitial fibrosis in a mineralocorticoid receptor-dependent fashion (Figures 2–4). Spironolactone treatment with modest BP reduction (Figure 1) almost completely abolished these abnormalities, suggesting that aldosterone acts perhaps via the receptor on the podocytes and mesangium in addition to that in tubules.[7–9,11–13] To note, an ARB olmesartan markedly ameliorated proteinuria and glomerular/podocyte injuries (Figures 2–6), suggesting that aldosterone activation of the RAAS in the kidney may have a causative role, especially in the absence of GC-A signaling. Several studies have provided evidence for positive feedback between aldosterone and the RAAS,[5–7] and GC-A knockout mice showed augmented angiotensin-converting enzyme and AT1 mRNA expression.[30] Activated AT1 signaling at podocytes would be sufficient to cause proteinuria and glomerular injury.[31,32] Furthermore, the crosstalk between AngII and GC-A signaling was shown in cultured podocytes.[33] These data suggest that lack of GC-A in the kidney should have a critical role in exaggerated activation of the "local" RAAS, which was abrogated by ARB treatment.

Aldosterone increases ROS production in the kidney.[7,8,12] This study reveals that the glomerular expression of gp91phox, a prototype of Nox family,[29] was upregulated in aldosterone-infused GC-A knockout mice (Figure 7). Treatment with tempol, a membrane-permeable radical scavenger,[8] inhibited such increases together with significant amelioration in nephropathy (Figures 2–6), suggesting the importance of ROS in this model. Thus far, little is known on the relationship between natriuretic peptides and ROS in renal injury. It has been reported that ANP counteracts ROS generation in aortic smooth muscle cells,[34] and inhibits ROS-induced cell damage

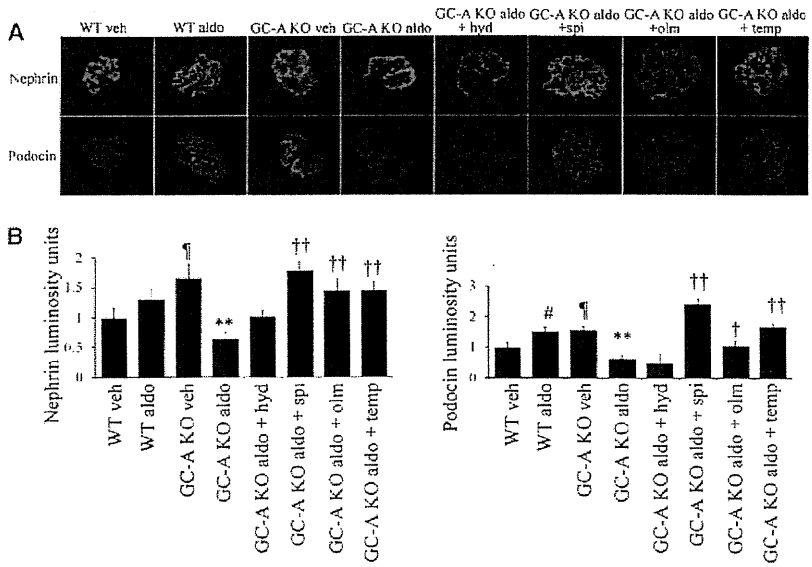

Figure 6. Immunostaining for nephrin and podocin. (A) Aldosterone-infused wild-type mice (WT aldo) showed normal linear staining for nephrin and podocin. Aldosterone-infused GC-A knockout mice (GC-A KO aldo) exhibited decreased expression of nephrin and podocin at 4 weeks. The expression of both nephrin and podocin was recovered by administration with spironolactone (GC-A KO aldo+spi), olmesartan (GC-A KO aldo+olm), or tempol (GC-A KO aldo+temp), but not with hydralazine (GC-A KO aldo+hyd). (B) Quantification of the mean intensity and the area of fluorescent staining for nephrin and podocin, and the products of multiplying the intensity and the area are shown. WT veh, n=5; WT aldo, n=8; KO veh, n=5; KO aldo, n=8; KO aldo+hyd, n=6; KO aldo+spi, n=5; KO aldo+olm, n=5; and KO aldo+temp, n=5. #P<0.05, WT veh versus WT aldo, **P<0.01, KO veh versus KO aldo, $^{\dagger}P$<0.05, $^{\dagger\dagger}P$<0.01, versus KO aldo, $^{\P}P$<0.05, KO veh versus WT veh. WT, wild-type; veh, vehicle; aldo, aldosterone; KO, knockout; hyd, hydralazine; spi, spironolactone; olm, olmesartan; temp, tempol.

via the GC-A/cGMP pathway.[35] The role of ROS in renal injury has been extensively studied,[36] and redox control is crucial in the pathophysiology of human and rodent diabetic nephropathy.[37,38] In this study, aldosterone caused increased glomerular expression of ROS- and ECM-related genes both in knockout and control mice. However, augmented 8-OHdG, massive proteinuria, and fibrotic changes occurred only in GC-A knockout mice, suggesting that, in wild-type mice, GC-A signaling may hamper intracellular mechanisms downstream of ROS signal against disease progression.

ROS-induced cell injury is mediated in part by the activation of MAPKs.[8,9] p38 MAPK plays a critical role in inflammation,[39] cytoskeleton stability,[40] and podocyte function.[41] We previously showed that inhibition of p38 MAPK markedly ameliorates podocyte injury and proteinuria in rodent models of nephrotic syndrome.[41] In this study, knockout mice with aldosterone exhibited augmented phosphorylation of p38 MAPK in podocytes, which was inhibited by RAAS blockade as well as tempol (Figure 8). In addition, ANP suppressed p38 MAPK phosphorylation, which was increased by GC-A knockdown in cultured podocytes (Figure 9, Supplemental Figure 4). Moreover, upregulation of connexin43, one of the earliest podocyte injury markers,[42] was induced by aldosterone and reduced by p38 MAPK inhibition (Figure 9E). It is thus conceivable that GC-A deficiency facilitated aldosterone- and ROS-induced activation of p38 MAPK, causing pronounced podocyte damage. It has been reported that ANP inhibits ROS-mediated p38 MAPK activation in lung endothelial cells.[43]

This study also demonstrated the enhanced ERK phosphorylation at podocytes in aldosterone-infused GC-A knockout mice, which was attenuated with RAAS blockade. We previously showed that natriuretic peptides prevent glomerular ERK activation in anti-GBM GN[25] and ameliorate AngII-induced cardiac hypertrophy and fibrosis.[44] *In vitro*, ANP and cGMP analog inhibited aldosterone-induced ERK phosphorylation (Figure 9), suggesting that natriuretic peptide/GC-A/cGMP pathway can counteract the activation of both MAPK pathways (Supplemental Figure 5).

This study provides an idea that suppression of GC-A signaling would be a potential risk for proteinuria under high aldosterone state. Impaired GC-A signaling can often be seen in chronic heart failure (natriuretic peptide resistance), in which RAAS activation would inevitably occur both systemically and locally.[45] Such conditions are well recognized as potentially harmful to the kidney, and supplementation of ANP or BNP could become a therapeutic option against disease progression.

In summary, this study reveals that aldosterone causes massive proteinuria and podocyte injury in the absence of GC-A signaling with the activation of ROS and MAPKs, and that RAAS blockade and ROS inhibition could ameliorate these abnormalities. These findings suggest that local inhibition of the RAAS and oxidative stress in podocytes may be a novel mechanism involved in the pleiotropic and renoprotective properties of endogenous natriuretic peptide/GC-A system.

CONCISE METHODS

Reagents and Antibodies

Aldosterone was obtained from Sigma Aldrich (St. Louis, MO). Reagents used were hydralazine (Sigma Aldrich), spironolactone (Sigma Aldrich), olmesartan (a gift from Daiichi Sankyo Pharmaceutical, Tokyo, Japan), tempol (Sigma Aldrich), MEK inhibitor U0126 (Cell Signaling Technology, Boston, MA), p38 MAPK inhibitor SB203580 (Cell Signaling Technology), and glucocorticoid receptor blocker mifepristone (Sigma Aldrich). Primary antibodies used for

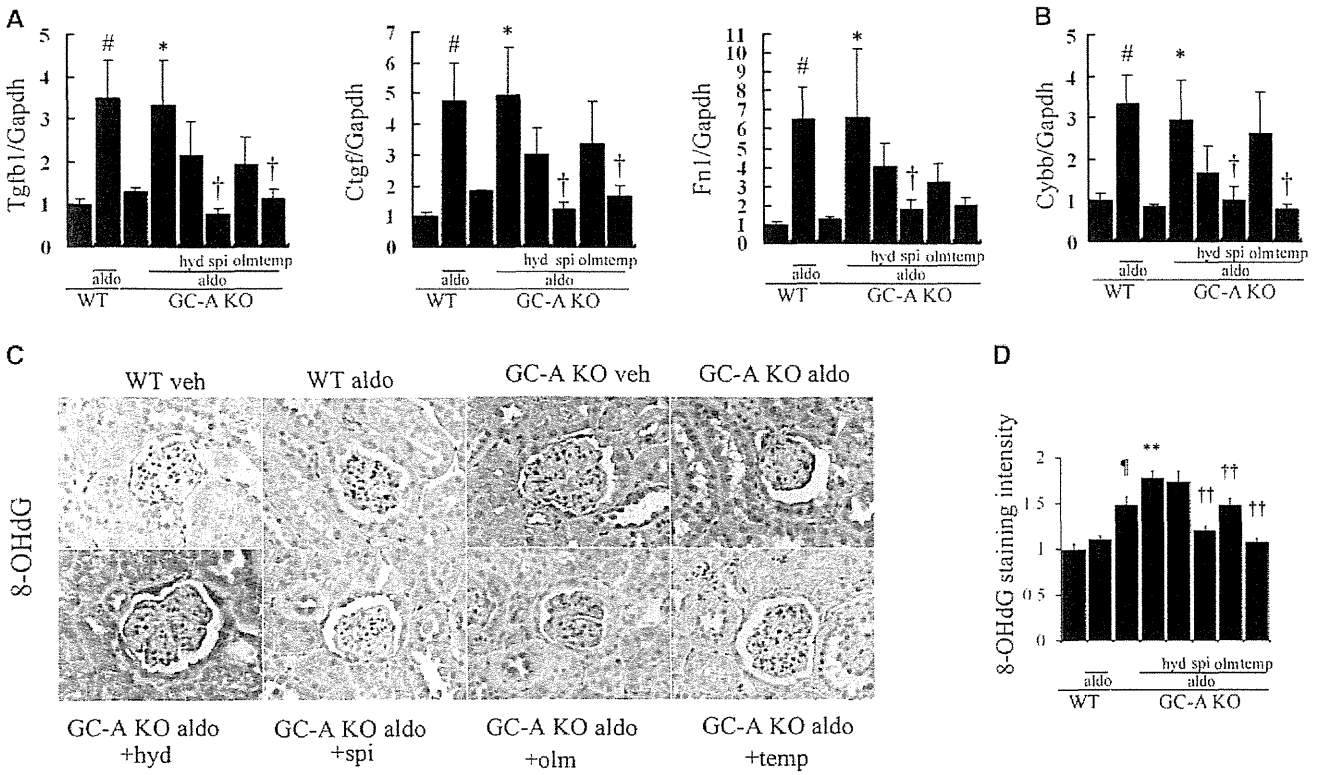

Figure 7. Glomerular mRNA expression at 4 weeks after aldosterone administration and ROS. (A, B) Real-time RT-PCR analyses of TGF-β1 (Tgfb1), connective tissue growth factor (Ctgf), fibronectin (Fn1), and gp91phox (Cybb) are shown. GAPDH mRNA expression is used as the control. (C) Immunohistochemical study for 8-OHdG. Aldosterone-infused wild-type mice (WT aldo) did not show the increase of 8-OHdG. Strong staining of 8-OHdG was detected in vehicle-infused GC-A knockout mice (GC-A KO veh), and aldosterone infusion (GC-A KO aldo) augmented 8-OHdG staining mainly at podocytes and tubular cells. Staining of 8-OHdG was reduced by administration with spironolactone (GC-A KO aldo+spi), olmesartan (GC-A KO aldo+olm), or tempol (GC-A KO aldo+temp), but not with hydralazine (GC-A KO aldo+hyd). (D) Quantification of the mean intensity of staining for 8-OHdG. WT veh, n=5; WT aldo, n=8; KO veh, n=5; KO aldo, n=8; KO aldo+hyd, n=6; KO aldo+spi, n=5; KO aldo+olm, n=5; and KO aldo+temp, n=5. $^{\#}P<0.05$, WT veh versus WT aldo,$^{*}P<0.05$, $^{**}P<0.01$, KO veh versus KO aldo, $^{\dagger}P<0.05$, $^{\dagger\dagger}P<0.01$, versus KO aldo, $^{\P}P<0.05$, KO veh versus WT veh. WT, wild-type; veh, vehicle; aldo, aldosterone; KO, knockout; hyd, hydralazine; spi, spironolactone; olm, olmesartan; temp, tempol.

Western blotting and immunohistochemical studies were goat anti-nephrin (R&D Systems, Minneapolis, MN), rabbit anti-podocin (Sigma Aldrich), rabbit anti-p44/42 MAPK, rabbit anti-phospho-p44/42 MAPK, rabbit anti-p38 MAPK, rabbit anti-phospho-p38 MAPK (Cell Signaling Technology), and goat anti-8-OHdG (Millipore, Temecula, CA) antibodies.

Animal Experiments

All animal experiments were approved by the Animal Experimentation Committee of Kyoto University Graduate School of Medicine. Mice deficient in GC-A were produced on 129/SVJ background[19] and then backcrossed with C57BL/6J mice more than 10 times. Male GC-A knockout mice or their wild-type littermates (approximately 28 g) received a left uninephrectomy or sham operation under intraperitoneal pentobarbital anesthesia (at −2 weeks). At 2 weeks after uninephrectomy or sham operation, an osmotic minipump (model 2004; Alzet, Cupertino, CA) was implanted subcutaneously to infuse vehicle or aldosterone (at 0 weeks). All mice were fed a diet containing 6% NaCl. Mice were assigned randomly to treated or untreated groups for 4 weeks: group 1, vehicle (2% ethanol)–infused wild-type mice (n=5); group 2, aldosterone (0.2 μg/kg body weight per minute)–infused wild-type mice (n=8); group 3, vehicle-infused GC-A knockout mice (n=5); group 4, aldosterone-infused GC-A knockout mice (n=8); group 5, aldosterone-infused GC-A knockout mice with hydralazine (60 mg/kg per day, in drinking water) (n=6); group 6, aldosterone-infused GC-A knockout mice with spironolactone (30 mg/kg per day, in drinking water) (n=5); group 7, aldosterone-infused GC-A knockout mice with olmesartan (10 mg/kg per day, in drinking water) (n=5); and group 8, aldosterone-infused GC-A knockout mice with tempol (110 mg/kg per day, in drinking water) (n=5).

Animals were given water *ad libitum*. BP was measured in conscious mice by the tail-cuff method (MK-2000ST; Muromachi Kikai, Tokyo, Japan) at −2, 0, 1, 2, and 4 weeks.[25] For urine measurements, each animal was housed separately in a metabolic cage (Shinano Manufacturing, Tokyo, Japan) at −2, 0, 1, 2, and 4 weeks.[46] Blood and kidney samples were harvested at 4 weeks. Glomeruli were isolated by the graded sieving method.[46] Urinary and serum creatinine were measured by the enzymatic method (SRL, Tokyo, Japan).[46] Serum aldosterone was measured by RIA (SRL). Urinary albumin excretion was assayed with a murine albumin ELISA kit (Exocell, Philadelphia, PA).[46]

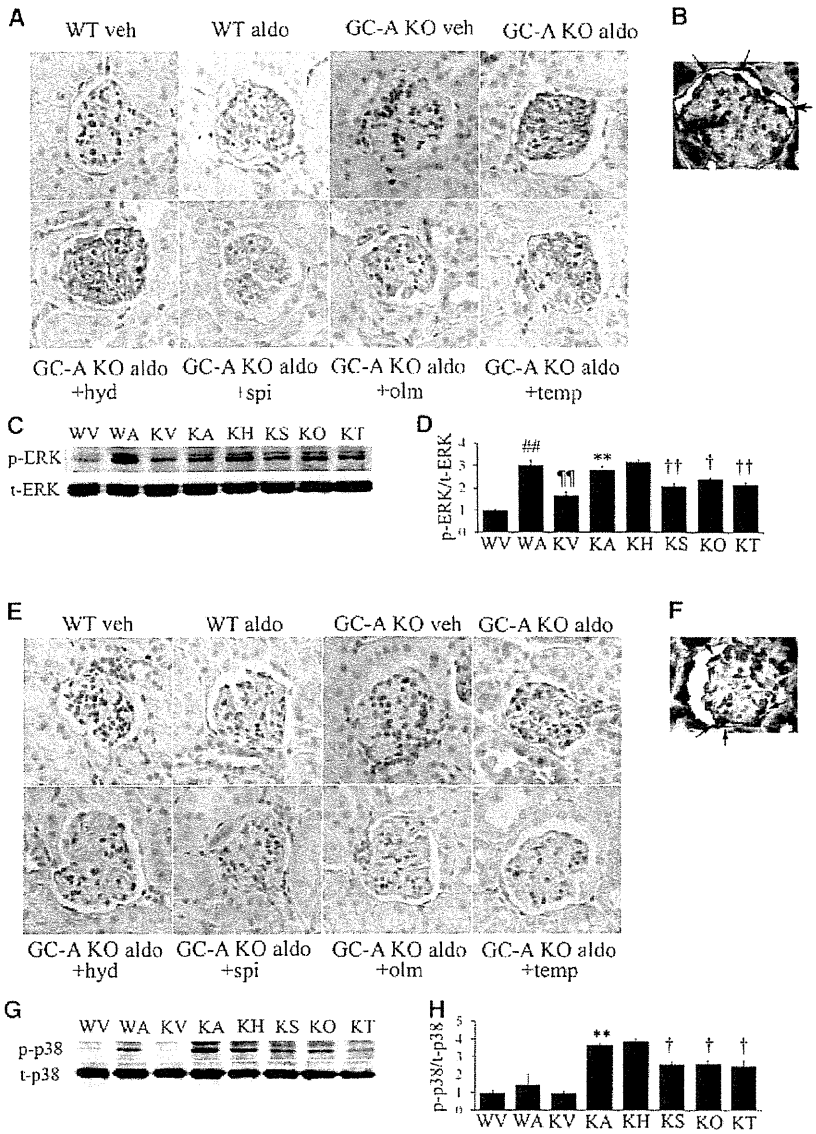

Figure 8. Enhanced phosphorylation of ERK and p38 MAPK in glomeruli of aldosterone-infused GC-A knockout mice. (A) Immunohistochemical study for phospho-ERK at 4 weeks after aldosterone infusion. (B) Double immunostaining for phospho-ERK (brown) and Wilms' tumor 1 (WT1, blue). Arrows indicate double positive cells. (C) Western blotting for phospho-ERK and total ERK in glomeruli of mice. (D) Quantification of relative phospho-ERK to total ERK levels analyzed with densitometer. (E) Immunohistochemical study for phospho-p38 MAPK at 4 weeks after aldosterone infusion. (F) Double immunostaining for phospho-p38 MAPK (brown) and WT1 (blue). Arrows indicate double positive cells. (G) Western blotting for phospho-p38 MAPK and total p38 MAPK in glomeruli of mice. (H) Quantification of relative phospho-p38 MAPK to total p38 MAPK levels analyzed with densitometer. n=3, each. $^{\#\#}P<0.01$, WT veh versus WT aldo, $^{**}P<0.01$, KO veh versus KO aldo, $^{\dagger}P<0.05$, $^{\dagger\dagger}P<0.01$, versus KO aldo, $^{\P\P}P<0.01$, KO veh versus WT veh. WT, wild-type; veh, vehicle; aldo, aldosterone; KO, knockout; hyd, hydralazine; spi, spironolactone; olm, olmesartan; temp, tempol; WV, wild-type mice with vehicle; WA, wild-type mice with aldosterone; KV, GC-A KO mice with vehicle; KA, GC-A KO mice with aldosterone; KH, GC-A KO mice with aldosterone treated with hydralazine; KS, GC-A KO mice with aldosterone treated with spironolactone; KO, GC-A KO mice with aldosterone treated with olmesartan; KT, GC-A KO mice with aldosterone treated with tempol.

Renal Histology and Electron Microscopy

Histologic and electron microscopic examinations were performed as described previously.[46,47] Briefly, kidney sections stained with periodic acid–Schiff were examined by light microscopy (IX-81; Olympus, Tokyo, Japan). The cross-sectional area and the mesangial area in both 10 superficial and 10 juxtamedullary glomeruli were measured quantitatively using a computer-aided manipulator (MetaMorph software; Molecular Devices, Sunnyvale, CA).[46] The number of sclerotic and all juxtaglomerular glomeruli was counted. The fibrotic area was also measured in Masson's trichrome-stained kidney sections quantitatively using a computer-aided manipulator (MetaMorph software).[47] Electron microscopic examination was performed in an electron microscope (H-7600; Hitachi, Tokyo, Japan). GBM thickness and foot process width were measured with Image J software (http://rsbweb.nih.gov/ij/; n=3, each). These procedures were performed by two investigators blinded to the origin of the slides and photos, and the mean values were calculated.

Immunohistochemistry

Immunofluorescence analyses for nephrin and podocin were described previously.[41,46] Briefly, cryostat sections were incubated with goat anti-nephrin antibody or rabbit anti-podocin antibody, and then incubated with FITC-labeled secondary antibodies (Jackson ImmunoResearch, West Grove, PA). Positive area and mean fluorescent intensity were measured with Image J software (n=3, each). Immunohistochemical studies for phospho-ERK, phospho-p38 MAPK, and 8-OHdG were also performed as previously described.[41] Briefly, paraffin-embedded sections were incubated with rabbit anti-phospho-p44/42 MAPK (ERK) antibody, rabbit anti-phospho-p38 MAPK antibody, or goat anti-8-OHdG antibody, and then incubated with horseradish peroxidase–labeled anti-rabbit or anti-goat antibodies (Jackson ImmunoResearch). Mean staining intensity was measured with Image J software (n=3, each). The sections were developed with 3,3'-diaminobenzidine tetrahydrochloride. WT1 immunostaining was performed as described.[46] For immunohistochemical studies for GC-A, paraffin-embedded, autoclave-heated sections were treated with 3% H_2O_2 and a biotin blocking kit (Vector Laboratories, Burlingame, CA), and were incubated with 10% normal goat serum in

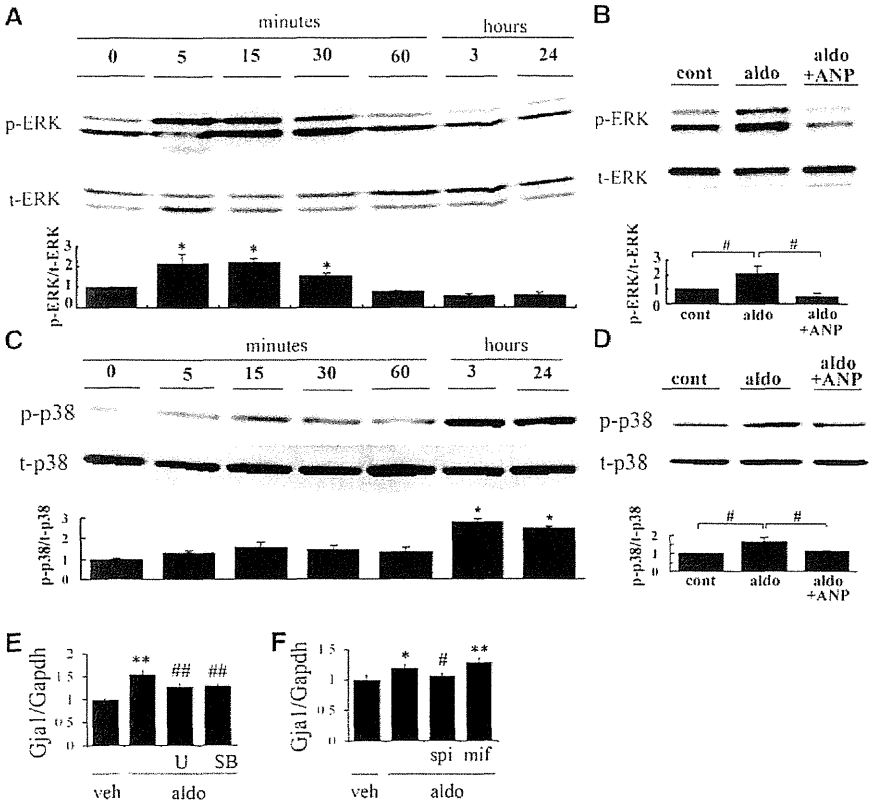

Figure 9. Aldosterone-induced phosphorylation of ERK and p38 MAPK in cultured mouse podocytes. (A) Time course of phospho-ERK and total ERK protein after administration of aldosterone (1 μM) in cultured podocytes. *P<0.01, versus 0 minutes. n=5. (B) Inhibitory effects of ANP (1 μM) on aldosterone-induced ERK phosphorylation. ANP (aldo+ANP) or vehicle (aldo) was administered 30 minutes before aldosterone or vehicle (cont) stimulation (1 μM). Cells were harvested at 10 minutes after aldosterone stimulation. #P<0.01. n=5. (C) Time course of phospho-p38 MAPK and total p38 MAPK protein after administration of aldosterone (1 μM) in cultured podocytes. *P<0.01, versus 0 minutes. n=5. (D) Inhibitory effects of ANP (1 μM) on aldosterone-induced p38 MAPK phosphorylation at 3 hours. Mean ± SEM *P<0.01, versus 0 minutes. #P<0.01. n=5. *P<0.01, versus 0 minutes. #P<0.01. n=5. (E) Inhibitory effects of MEK inhibitor or p38 MAPK inhibitor on connexin43 (Gja1) mRNA expression in mouse podocytes. U, U0126 (10 μM); SB, SB203580 (10 μM). **P<0.01 versus veh. ##P<0.01 versus aldosterone. n=3. (F) Glucocorticoid receptor blocker, mifepristone, did not reduce aldosterone-induced connexin43 expression. Spi, spironolactone (10 μM), mifepristone (10 μM). *P<0.05, **P<0.01 versus veh, #P<0.05 versus aldosterone. n=3. WT, wild-type; veh, vehicle; aldo, aldosterone; KO, knockout; hyd, hydralazine; spi, spironolactone; olm, olmesartan; temp, tempol.

PBS. The sections were incubated with rabbit anti-NPR-A (GC-A) antibody (Santa Cruz Biotechnology, Santa Cruz, CA) diluted 1:20 in PBS for 1 hour at room temperature, and then incubated with goat biotin-conjugated anti-rabbit antibody (Vector Laboratories). The sections were processed with LSAB2 streptavidin-HRP (DAKO, Glostrup, Denmark), and developed with 3,3′-diaminobenzidine tetrahydrochloride.

Glomerular RNA Extraction and Real-Time RT-PCR Analyses

Quantitative real-time RT-PCR was performed using the StepOnePlus system (Applied Biosystems, Foster City, CA) as described previously.[46] TGF-β1, COL1A1, COL4A3, fibronectin, gp91phox/Cybb (Nox-2), p22phox/Cyba, and Nox-4 mRNA expressions were evaluated. Some of primers and probe sets were described elsewhere[46] and included the following: COL1A1 forward primer, 5′-gtcccaacccccaaagac-3′; COL1A1 reverse primer, 5′-catcttctgagtttggtgatacgt-3′; COL1A1 probe, 5′-FAM-tgctgtgctttctgcccgga-TAMRA-3′; Cybb forward primer, 5′-ggtgacaatgagaacgaagagtatc-3′; Cybb reverse primer, 5′-gagacacagtgtgatgacaattcc-3′; Cybb probe, 5′-FAM-cagccaaccgagtcacggccacatac-TAMRA-3′; Cyba forward primer, 5′-cccctcaccaggaattactacg-3′; Cyba reverse primer, 5′-cactgctcacctcggatgg-3′; Cyba probe, 5′-FAM-ctccacttcctgttgtcggtgcctgc-TAMRA-3′; Nox-4 forward primer, 5′-gcaagactctacacatcacatgtg-3′; Nox-4 reverse primer, 5′-tgctgcattcagttcaaggaaatc-3′; Nox-4 probe, 5′-FAM-tctcaggtgtgcatgtagccgccca-TAMRA-3′; Gja1 forward primer, 5′-ctctccttttccttttgacttcagc-3′; Gja1 reverse primer, gaccttgtccagcagcttcc; and Gja1 probe, 5′-FAM-aaggagttccaccactttggcgtgcc-TAMRA-3′. Expression of each mRNA was normalized with GAPDH mRNA (TaqMan rodent GAPDH control reagents; Applied Biosystems).

Cell Cultures

A conditionally immortalized mouse podocyte cell line was provided by Dr. Peter Mundel (University of Miami Miller School of Medicine, Miami, FL) and cultured as described.[41] For time-course experiments, differentiated podocytes were made quiescent in medium that contained 0.1% FBS for 24 hours, and then cells were stimulated with 1 μM aldosterone and further incubated for a period ranging from 5 minutes to 24 hours. The effect of ANP (Peptide Institute, Osaka, Japan) on phosphorylation of ERK and p38 MAPK was studied in the presence of aldosterone. Cells were made quiescent in medium that contained 0.1% FBS for 24 hours, pretreated with 1 μM ANP or vehicle (final 0.005% glucose solution) 30 minutes before stimulation with 1 μM aldosterone or vehicle (final 0.2% ethanol), and then harvested at 10 minutes or 3 hours after stimulation for ERK and p38 MAPK analyses, respectively.

Connexin43 (Gja1) mRNA expression was evaluated by TaqMan PCR. Differentiated podocytes were made quiescent, pretreated with 10 μM U0126 or 10 μM SB203580 for 30 minutes, and then stimulated with 1 μM aldosterone. Cells were harvested at 24 hours after stimulation with a RNeasy Mini kit (Qiagen). For analysis of the glucocorticoid pathway, cells were pretreated with 10 μM mifepristone or 10 μM spironolactone and were harvested at 3 hours after aldosterone (1 μM) stimulation.

Western Blot Analyses

Western blot analysis was performed as described.[46,47] Briefly, isolated glomeruli were homogenized in cold RIPA buffer (50 mM Tris-HCl, 150 mM NaCl, 4 mM EDTA, 1% Nonidet P-40, 0.1% sodium deoxycholate, 10 mM $Na_4P_2O_7$, 10 mM NaF, 10 μg/ml aprotinin, 2 mM dithiothreitol, 2 mM sodium orthovanadate, and 1 mM PMSF). For cultured cells, cells were lysed with RIPA buffer for ERK detection, or were processed with the AllPrep DNA/RNA/protein Mini kit and then lysed with lysis buffer containing 100 mM Tris-HCl, 3% SDS, 10 mM $NaHPO_4$, 1% Nonidet P-40, 20 mM EDTA, 10 μg/ml aprotinin, 2 mM dithiothreitol, 2 mM sodium orthovanadate, and 1 mM PMSF for p38 MAPK detection. The homogenates were centrifuged at 15,000 rpm for 15 minutes at 4°C, and the supernatants were treated with NuPAGE sample buffer (Invitrogen, Carlsbad, CA). Western blot analysis was performed as described with some modifications using NuPAGE Bis-Tris gels (Invitrogen).[47] Filters on isolated cell extracts were incubated with rabbit anti-phospho-p44/p42 MAPK antibody or anti-phospho-p38 MAPK antibody for 1 hour, and immunoblots were developed using horseradish peroxidase-linked donkey anti-rabbit antibodies (Amersham, Arlington Heights, IL) and a chemiluminescence kit (Amersham).

Statistical Analyses

Data are expressed as the mean ± SEM. Statistical analysis was performed using one-way ANOVA. $P<0.05$ was considered statistically significant.

ACKNOWLEDGMENTS

We gratefully acknowledge Mr. M. Fujimoto and Mr. Y. Sakashita and other laboratory members for technical assistance and Ms. A. Yamamoto for secretarial assistance.

This work was supported in part by research grants from the Japanese Ministry of Education, Culture, Sports, Science, and Technology; the Japanese Ministry of Health, Labour, and Welfare; and the Salt Science Research Foundation.

DISCLOSURES

None.

REFERENCES

1. Nishimura M, Uzu T, Fujii T, Kuroda S, Nakamura S, Inenaga T, Kimura G: Cardiovascular complications in patients with primary aldosteronism. *Am J Kidney Dis* 33: 261–266, 1999
2. Schrier RW, Masoumi A, Elhassan E: Aldosterone: Role in edematous disorders, hypertension, chronic renal failure, and metabolic syndrome. *Clin J Am Soc Nephrol* 5: 1132–1140, 2010
3. Ribstein J, Du Cailar G, Fesler P, Mimran A: Relative glomerular hyperfiltration in primary aldosteronism. *J Am Soc Nephrol* 16: 1320–1325, 2005
4. Greene EL, Kren S, Hostetter TH: Role of aldosterone in the remnant kidney model in the rat. *J Clin Invest* 98: 1063–1068, 1996
5. Klar J, Vitzthum H, Kurtz A: Aldosterone enhances renin gene expression in juxtaglomerular cells. *Am J Physiol Renal Physiol* 286: F349–F355, 2004
6. Harada E, Yoshimura M, Yasue H, Nakagawa O, Nakagawa M, Harada M, Mizuno Y, Nakayama M, Shimasaki Y, Ito T, Nakamura S, Kuwahara K, Saito Y, Nakao K, Ogawa H: Aldosterone induces angiotensin-converting-enzyme gene expression in cultured neonatal rat cardiocytes. *Circulation* 104: 137–139, 2001
7. Briet M, Schiffrin EL: Aldosterone: Effects on the kidney and cardiovascular system. *Nat Rev Nephrol* 6: 261–273, 2010
8. Nishiyama A, Yao L, Nagai Y, Miyata K, Yoshizumi M, Kagami S, Kondo S, Kiyomoto H, Shokoji T, Kimura S, Kohno M, Abe Y: Possible contributions of reactive oxygen species and mitogen-activated protein kinase to renal injury in aldosterone/salt-induced hypertensive rats. *Hypertension* 43: 841–848, 2004
9. Terada Y, Kobayashi T, Kuwana H, Tanaka H, Inoshita S, Kuwahara M, Sasaki S: Aldosterone stimulates proliferation of mesangial cells by activating mitogen-activated protein kinase 1/2, cyclin D1, and cyclin A. *J Am Soc Nephrol* 16: 2296–2305, 2005
10. Mundel P, Reiser J: Proteinuria: An enzymatic disease of the podocyte? *Kidney Int* 77: 571–580, 2010
11. Nagase M, Shibata S, Yoshida S, Nagase T, Gotoda T, Fujita T: Podocyte injury underlies the glomerulopathy of Dahl salt-hypertensive rats and is reversed by aldosterone blocker. *Hypertension* 47: 1084–1093, 2006
12. Shibata S, Nagase M, Yoshida S, Kawachi H, Fujita T: Podocyte as the target for aldosterone: Roles of oxidative stress and Sgk1. *Hypertension* 49: 355–364, 2007
13. Shibata S, Nagase M, Yoshida S, Kawarazaki W, Kurihara H, Tanaka H, Miyoshi J, Takai Y, Fujita T: Modification of mineralocorticoid receptor function by Rac1 GTPase: Implication in proteinuric kidney disease. *Nat Med* 14: 1370–1376, 2008
14. Nakao K, Ogawa Y, Suga S, Imura H: Molecular biology and biochemistry of the natriuretic peptide system. I: Natriuretic peptides. *J Hypertens* 10: 907–912, 1992
15. Sugawara A, Nakao K, Morii N, Yamada T, Itoh H, Shiono S, Saito Y, Mukoyama M, Arai H, Nishimura K, Obata K, Yasue H, Ban T, Imura H: Synthesis of atrial natriuretic polypeptide in human failing hearts. Evidence for altered processing of atrial natriuretic polypeptide precursor and augmented synthesis of β-human ANP. *J Clin Invest* 81: 1962–1970, 1988
16. Mukoyama M, Nakao K, Hosoda K, Suga S, Saito Y, Ogawa Y, Shirakami G, Jougasaki M, Obata K, Yasue H, Kambayashi Y, Inouye K, Imura H: Brain natriuretic peptide as a novel cardiac hormone in humans. Evidence for an exquisite dual natriuretic peptide system, atrial natriuretic peptide and brain natriuretic peptide. *J Clin Invest* 87: 1402–1412, 1991
17. Potter LR, Abbey-Hosch S, Dickey DM: Natriuretic peptides, their receptors, and cyclic guanosine monophosphate-dependent signaling functions. *Endocr Rev* 27: 47–72, 2006
18. Ritter D, Dean AD, Gluck SL, Greenwald JE: Natriuretic peptide receptors A and B have different cellular distributions in rat kidney. *Kidney Int* 48: 5758–5766, 1995
19. Lopez MJ, Wong SK, Kishimoto I, Dubois S, Mach V, Friesen J, Garbers DL, Beuve A: Salt-resistant hypertension in mice lacking the guanylyl cyclase-A receptor for atrial natriuretic peptide. *Nature* 378: 65–68, 1995
20. Kishimoto I, Rossi K, Garbers DL: A genetic model provides evidence that the receptor for atrial natriuretic peptide (guanylyl cyclase-A) inhibits cardiac ventricular myocyte hypertrophy. *Proc Natl Acad Sci USA* 98: 2703–2706, 2001
21. Kishimoto I, Dubois SK, Garbers DL: The heart communicates with the kidney exclusively through the guanylyl cyclase-A receptor: Acute handling of sodium and water in response to volume expansion. *Proc Natl Acad Sci USA* 93: 6215–6219, 1996

22. Conger JD, Falk SA, Hammond WS: Atrial natriuretic peptide and dopamine in established acute renal failure in the rat. *Kidney Int* 40: 21–28, 1991
23. Nigwekar SU, Navaneethan SD, Parikh CR, Hix JK: Atrial natriuretic peptide for management of acute kidney injury: A systematic review and meta-analysis. *Clin J Am Soc Nephrol* 4: 261–272, 2009
24. Kasahara M, Mukoyama M, Sugawara A, Makino H, Sugamami T, Ogawa Y, Nakagawa M, Yahata K, Goto M, Ishibashi R, Tamura N, Tanaka I, Nakao K: Ameliorated glomerular injury in mice overexpressing brain natriuretic peptide with renal ablation. *J Am Soc Nephrol* 11: 1691–1701, 2000
25. Suganami T, Mukoyama M, Sugawara A, Mori K, Nagae T, Kasahara M, Yahata K, Makino H, Fujinaga Y, Ogawa Y, Tanaka I, Nakao K: Overexpression of brain natriuretic peptide in mice ameliorates immune-mediated renal injury. *J Am Soc Nephrol* 12: 2652–2663, 2001
26. Makino H, Mukoyama M, Mori K, Suganami T, Kasahara M, Yahata K, Nagae T, Yokoi H, Sawai K, Ogawa Y, Suga S, Yoshimasa Y, Sugawara A, Tanaka I, Nakao K: Transgenic overexpression of brain natriuretic peptide prevents the progression of diabetic nephropathy in mice. *Diabetologia* 49: 2514–2524, 2006
27. Opgenorth TJ, Burnett JC Jr, Granger JP, Scriven TA: Effects of atrial natriuretic peptide on renin secretion in nonfiltering kidney. *Am J Physiol* 250: F798–F801, 1986
28. Ito T, Yoshimura M, Nakamura S, Nakayama M, Shimasaki Y, Harada E, Mizuno Y, Yamamuro M, Harada M, Saito Y, Nakao K, Kurihara H, Yasue H, Ogawa H: Inhibitory effect of natriuretic peptides on aldosterone synthase gene expression in cultured neonatal rat cardiocytes. *Circulation* 107: 807–810, 2003
29. Bedard K, Krause KH: The NOX family of ROS-generating NADPH oxidases: Physiology and pathophysiology. *Physiol Rev* 87: 245–313, 2007
30. Vellaichamy E, Zhao D, Somanna N, Pandey KN: Genetic disruption of guanylyl cyclase/natriuretic peptide receptor-A upregulates ACE and AT1 receptor gene expression and signaling: Role in cardiac hypertrophy. *Physiol Genomics* 31: 193–202, 2007
31. Hoffmann S, Podlich D, Hähnel B, Kriz W, Gretz N: Angiotensin II type 1 receptor overexpression in podocytes induces glomerulosclerosis in transgenic rats. *J Am Soc Nephrol* 15: 1475–1487, 2004
32. Crowley SD, Vasievich MP, Ruiz P, Gould SK, Parsons KK, Pazmino AK, Facemire C, Chen BJ, Kim HS, Tran TT, Pisetsky DS, Barisoni L, Prieto-Carrasquero MC, Jeansson M, Foster MH, Coffman TM: Glomerular type 1 angiotensin receptors augment kidney injury and inflammation in murine autoimmune nephritis. *J Clin Invest* 119: 943–953, 2009
33. Golos M, Lewko B, Bryl E, Witkowski JM, Dubaniewicz A, Olszewska A, Latawiec E, Angielski S, Stepinski J: Effect of angiotensin II on ANP-dependent guanylyl cyclase activity in cultured mouse and rat podocytes. *Kidney Blood Press Res* 25: 296–302, 2002
34. Baldini PM, De Vito P, D'aquilio F, Vismara D, Zalfa F, Bagni C, Fiaccavento R, Di Nardo P: Role of atrial natriuretic peptide in the suppression of lysophosphatydic acid-induced rat aortic smooth muscle (RASM) cell growth. *Mol Cell Biochem* 272: 19–28, 2005
35. Bilzer M, Jaeschke H, Vollmar AM, Paumgartner G, Gerbes AL: Prevention of Kupffer cell-induced oxidant injury in rat liver by atrial natriuretic peptide. *Am J Physiol* 276: G1137–G1144, 1999
36. Modlinger PS, Wilcox CS, Aslam S: Nitric oxide, oxidative stress, and progression of chronic renal failure. *Semin Nephrol* 24: 354–365, 2004
37. Pergola PE, Raskin P, Toto RD, Meyer CJ, Huff JW, Grossman EB, Krauth M, Ruiz S, Audhya P, Christ-Schmidt H, Wittes J, Warnock DG; BEAM Study Investigators: Bardoxolone methyl and kidney function in CKD with type 2 diabetes. *N Engl J Med* 365: 327–336, 2011
38. Jiang T, Huang Z, Lin Y, Zhang Z, Fang D, Zhang DD: The protective role of Nrf2 in streptozotocin-induced diabetic nephropathy. *Diabetes* 59: 850–860, 2010
39. Thalhamer T, McGrath MA, Harnett MM: MAPKs and their relevance to arthritis and inflammation. *Rheumatology (Oxford)* 47: 409–414, 2008
40. Kim EK, Choi EJ: Pathological roles of MAPK signaling pathways in human diseases. *Biochim Biophys Acta* 1802: 396–405, 2010
41. Koshikawa M, Mukoyama M, Mori K, Suganami T, Sawai K, Yoshioka T, Nagae T, Yokoi H, Kawachi H, Shimizu F, Sugawara A, Nakao K: Role of p38 mitogen-activated protein kinase activation in podocyte injury and proteinuria in experimental nephrotic syndrome. *J Am Soc Nephrol* 16: 2690–2701, 2005
42. Yaoita E, Yao J, Yoshida Y, Morioka T, Nameta M, Takata T, Kamiie J, Fujinaka H, Oite T, Yamamoto T: Up-regulation of connexin43 in glomerular podocytes in response to injury. *Am J Pathol* 161: 1597–1606, 2002
43. Stephens RS, Rentsendorj O, Servinsky LE, Moldobaeva A, Damico R, Pearse DB: cGMP increases antioxidant function and attenuates oxidant cell death in mouse lung microvascular endothelial cells by a protein kinase G-dependent mechanism. *Am J Physiol Lung Cell Mol Physiol* 299: L323–L333, 2010
44. Takahashi N, Saito Y, Kuwahara K, Harada M, Kishimoto I, Ogawa Y, Kawakami R, Nakagawa Y, Nakanishi M, Nakao K: Angiotensin II-induced ventricular hypertrophy and extracellular signal-regulated kinase activation are suppressed in mice overexpressing brain natriuretic peptide in circulation. *Hypertens Res* 26: 847–853, 2003
45. Schrier RW, Abraham WT: Hormones and hemodynamics in heart failure. *N Engl J Med* 341: 577–585, 1999
46. Yokoi H, Mukoyama M, Mori K, Kasahara M, Suganami T, Sawai K, Yoshioka T, Saito Y, Ogawa Y, Kuwabara T, Sugawara A, Nakao K: Overexpression of connective tissue growth factor in podocytes worsens diabetic nephropathy in mice. *Kidney Int* 73: 446–455, 2008
47. Yokoi H, Mukoyama M, Nagae T, Mori K, Suganami T, Sawai K, Yoshioka T, Koshikawa M, Nishida T, Takigawa M, Sugawara A, Nakao K: Reduction in connective tissue growth factor by antisense treatment ameliorates renal tubulointerstitial fibrosis. *J Am Soc Nephrol* 15: 1430–1440, 2004

This article contains supplemental material online at http://jasn.asnjournals.org/lookup/suppl/doi.10.1681/ASN.2011100985/-/DCSupplemental.

Ghrelin Prevents Incidence of Malignant Arrhythmia after Acute Myocardial Infarction through Vagal Afferent Nerves

Yuanjie Mao, Takeshi Tokudome, Kentaro Otani, Ichiro Kishimoto, Michio Nakanishi, Hiroshi Hosoda, Mikiya Miyazato, and Kenji Kangawa

Reprinted from Endocrinology Volume 153, Number 7

Ghrelin Prevents Incidence of Malignant Arrhythmia after Acute Myocardial Infarction through Vagal Afferent Nerves

Yuanjie Mao, Takeshi Tokudome, Kentaro Otani, Ichiro Kishimoto, Michio Nakanishi, Hiroshi Hosoda, Mikiya Miyazato, and Kenji Kangawa

Department of Biochemistry (Y.M., T.T., I.K., M.M., K.K.), Department of Regenerative Medicine and Tissue Engineering (K.O., H.H.), and Department of Cardiovascular Medicine (M.N.), National Cerebral and Cardiovascular Center, Suita, Osaka 565-8565, Japan

Ghrelin is a GH-releasing peptide mainly excreted from the stomach. Ghrelin administration has been shown to inhibit cardiac sympathetic nerve activity (CSNA), reduce malignant arrhythmia, and improve prognosis after acute myocardial infarction (MI). We therefore investigated the effects and potential mechanisms of the action of endogenous ghrelin on survival rate and CSNA after MI by using ghrelin-knockout (KO) mice. MI was induced by left coronary artery ligation in 46 KO mice and 41 wild-type mice. On the first day, malignant arrhythmia-induced mortality was observed within 30 min of the ligation and had an incidence of 2.4% in wild-type and 17.4% in KO mice ($P < 0.05$). We next evaluated CSNA by spectral analysis of heart rate variability. CSNA, represented by the low frequency/high frequency ratio, was higher in KO mice at baseline (2.18 ± 0.43 *vs.* 0.98 ± 0.09; $P < 0.05$), and especially after MI (25.5 ± 11.8 *vs.* 1.4 ± 0.3; $P < 0.05$), than in wild-type mice. Ghrelin (150 μg/kg, sc) 15 min before ligation suppressed the activation of CSNA and reduced mortality in KO mice. Further, this effect of ghrelin was inhibited by methylatropine bromide (1 mg/kg, ip) or by perineural treatment of both cervical vagal trunks with capsaicin (a specific afferent neurotoxin). Our data demonstrated that both exogenous and endogenous ghrelin suppressed CSNA, prevented the incidence of malignant arrhythmia, and improved the prognosis after acute MI. These effects are likely to be via the vagal afferent nerves. (***Endocrinology* 153: 3426–3434, 2012**)

Myocardial infarction (MI) is the most common cause of death in industrialized countries. In most cases, death occurs during the acute phase, *i.e.* the first 3–6 h after MI. This high mortality mainly results from malignant ventricular arrhythmia, which is strongly associated with an adverse and sustained increase in cardiac sympathetic nerve activity (CSNA) (1). Even for those who survive the immediate infarct, increased CSNA is also thought to contribute to left ventricular (LV) remodeling, which results in subsequent heart failure and mortality (2, 3). β-Adrenergic blockade, through the suppression of CSNA, has been shown to reduce the incidence of ventricular arrhythmia, attenuate the adverse ventricular remodeling, and decrease mortality after MI (2, 4).

Ghrelin is a GH-releasing peptide, originally isolated from the stomach in 1999, which has been identified as an endogenous ligand for the GH secretagogue receptor (GHS-R) (5). GHS-R mRNA is detected in not only the hypothalamus and pituitary but also the heart and blood vessels (6, 7), and much evidence for a cardiovascular function of ghrelin has been reported. Previous studies have revealed that chronic administration of exogenous ghrelin improved cardiac performance in rats and humans with chronic heart failure, as indicated by increases in cardiac output and LV fractional shortening (8, 9). Early ghrelin intervention also prevented the adverse increase in CSNA after acute MI, as well as reduced malignant ar-

ISSN Print 0013-7227 ISSN Online 1945-7170
Printed in U.S.A.

doi: 10.1210/en.2012-1065 Received January 18, 2012. Accepted April 12, 2012.
First Published Online April 25, 2012

Abbreviations: BP, Blood pressure; CSNA, cardiac sympathetic nerve activity; ECG, electrocardiography; GHS-R, GH secretagogue receptor; HF, high frequency; HR, heart rate; KO, ghrelin knockout; LF, low frequency; LV, left ventricular; MI, myocardial infarction; nHF, percentage of HF in total power; nLF, percentage of LF in total power; NTS, nucleus tractus solitarius; WT, wild type.